BACKMIXING IN A CYLINDRICAL CONFINED JET

GUNTER MOELLER

Submitted to the Faculty of Graduate Studies and Research of McGill University in partial fulfillment of the requirements for the degree of Master of Engineering

Thesis Supervisor : Dr. John M. Dealy

Department of Chemical Engineering
McGill University, Montreal, Canada

August, 1968

ABSTRACT

Recirculation or backflow is an interesting phenomenon that occurs in confined jets. In this study, the backmixing of fluid in a cylindrical confined jet was investigated. Residence time distributions were obtained by the transient response technique using pulse injections of a saturated salt solution. Tracer concentrations in the efflux of this system were measured conductimetrically. RTD data were collected for flows with and without the presence of a recirculation eddy. Certain features of the RTD curves are correlated with the similarity parameter, the Craya-Curtet number. A mixing model for the cylindrical confined jet is proposed.

The recirculation eddy was found to increase the mixedness of the fluid in this system, for Craya-Curtet numbers less than 0.80. At the same time, a considerable amount of dead space is formed within the recirculation eddy. Thus, it appears that the cylindrical confined jet is not practical for use as a mixing device.

ACKNOWLEDGEMENTS

The author wishes to express his sincere gratitude and appreciation to Dr. J. M. Dealy for his guidance, encouragement and valuable suggestions as director of this investigation.

The author is also thankful to :

The academic and technical staff of the Chemical Engineering Department for their invaluable help and advice.

The National Research Council and the Quebec Government for their financial assistance.

My wife for her constant encouragement, understanding, patience and typing ability.

TABLE OF CONTENTS

		PAGE
ABSTRACT		i
ACKNOWLEDGEMENTS		ii
TABLE OF CONTENTS		iii
LIST OF ILLUSTRATIONS		v
LIST OF TABLES		vii
I	INTRODUCTION	1
II	FLUID DYNAMICS OF CYLINDRICAL CONFINED JETS	3
III	A METHOD TO CHARACTERIZE THE MIXING PATTERNS IN A CLOSED VESSEL	9
	A. Introduction	9
	B. Age Distribution Functions	11
	C. Experimental Methods to Determine the Residence Time Distributions	13
	D. Interpretation of RTD Data	16
IV	LABORATORY STUDIES	20
	A. Introduction	20
	B. Apparatus	22
	C. Preliminary Studies	32
	D. Procedure	35
V	EXPERIMENTAL RESULTS	39
	A. Data Reduction	39
	B. Data Analysis and Presentation	45

		PAGE
VI	DISCUSSION OF RESULTS	63
VII	CONCLUSIONS AND RECOMMENDATIONS	77
NOMENCLATURE		79
REFERENCES		81
APPENDIX I		83
APPENDIX II		86

LIST OF ILLUSTRATIONS

		PAGE
FIGURE 1	RECIRCULATION EDDY	4
2	PROPERTIES OF THE E AND I CURVES FOR IDEAL FLOW PATTERNS IN CLOSED VESSELS	14
3	OVERALL VIEW OF THE APPARATUS	23
4	SCHEMATIC DIAGRAM OF THE EXPERIMENTAL EQUIPMENT	24
5	CLOSE-UP OF THE FLOW VESSEL	25
6	SECONDARY FLOW CONDITIONING CHAMBER	26
7	MIXING CHAMBER	28
8	THE INJECTION SYSTEM	30
9	THE CONDUCTIVITY PROBE	31
10	APPARATUS TO STUDY THE PULSE INJECTIONS AT THE END OF THE JET TUBE	36
11	RECORDER TRACE OF CONDUCTIVITY SHOWING THE PROCEDURE TO FIND t_o (C_t= 0.577)	40
12	RECORDER TRACE OF CONDUCTIVITY SHOWING MULTIPLE PEAKS (C_t= 0.577)	41
13	RECORDER TRACE OF CONDUCTIVITY MEASURED AT THE OUTLET OF THE JET TUBE FOR A FIXED REYNOLDS NUMBER	42

		PAGE
FIGURE 14	EFFECT OF THE CRAYA-CURTET NUMBER ON THE APPARENT PLUG FLOW RESIDENCE TIME	48
15	EFFECT OF THE CRAYA-CURTET NUMBER ON THE APPARENT PERFECT MIXING RESIDENCE TIME	51
16	EFFECT OF THE CRAYA-CURTET NUMBER ON THE PREDICTED MEAN RESIDENCE TIME	55
17	RTD CURVES OF THE CYLINDRICAL CONFINED JET FOR $C_t = 1.009$ AND $C_t = .510$	58
18	RTD CURVES OF THE CYLINDRICAL CONFINED JET FOR $C_t = .754$ AND $C_t = .631$	59
19	RTD CURVES OF THE CYLINDRICAL CONFINED JET SHOWING REPRODUCIBILITY (C_t=.875)	60
20	RTD CURVES OF THE CYLINDRICAL CONFINED JET WITH SMALLER MIXING VOLUME (C_t=1.009)	61
21	RTD CURVES OF THE CYLINDRICAL CONFINED JET WITH SMALLER MIXING VOLUME (C_t=.695)	62
22	SCHEMATIC DIAGRAM OF THE HYPOTHESIZED MIXING PROCESS IN A CYLINDRICAL CONFINED JET	73
23	SIMPLIFIED MIXING MODEL OF THE CYLINDRICAL CONFINED JET	76

LIST OF TABLES

		PAGE
TABLE 1	EXPERIMENTAL RESULTS FOR THE TIME DELAY t^*	47
2	EXPERIMENTAL RESULTS FOR THE EXPONENTIAL SLOPE S	50
3	PREDICTED MEAN RESIDENCE TIMES FOR THE CYLINDRICAL CONFINED JET ACCORDING TO DATA BY BARCHILON AND CURTET	54
4	COMPARISON OF ESTIMATED AND CALCULATED MEAN RESIDENCE TIMES	56

1

INTRODUCTION

A jet is formed when a high velocity stream of fluid discharges into a surrounding low velocity stream. When a jet issues into a vessel such that the solid boundaries of this vessel have an important effect on the development of the jet, it is called a confined jet. Such jets have important applications in jet pumps, jet ejectors, jet flame furnaces, mixing tanks and more recently in fluidic amplifiers (15).

Confined incompressible jets have received considerable attention in the past decade from the fluid mechanics point of view. Velocity and pressure profiles have been measured for a wide range of jet Reynolds numbers and ratios of jet to mixing tube diameters. Some theoretical work has been done to predict these profiles. The results of the above work have led to the establishment of a dimensionless similarity parameter called the Craya-Curtet number, C_t, which characterizes the flow regime in a confined jet. In particular, this parameter which depends only on the boundary conditions of the system, has been shown to govern the onset of recirculation, a phenomenon of great significance in the mixing of the two fluid streams.

The object of this research was to conduct a macroscopic study of the axial mixing in a cylindrical confined jet in the realm of recirculatory and non-recirculatory flows. This was achieved by obtaining the residence time distributions, RTD, for this system by the transient response technique using pulse injections. It was also of interest to relate the known fluid mechanics to these distributions. This would enable one to establish a mixing model for this system corresponding in detail to the existing flow patterns. This is important if such a model is to be used to predict the performance of non-linear processes accurately.

Experimentally, a shot of conductive salt was injected into the jet stream to serve as the tracer. The mixing tube efflux passed through a conductivity probe whose output was continuously monitored and recorded. The fluid in both jet and secondary streams was plain tap water.

Some RTD curves are presented and some features of these curves are correlated with respect to the Craya-Curtet number. A mixing model is proposed for the cylindrical confined jet on the basis of experimental evidence and known fluid dynamics of this system.

II

FLUID DYNAMICS OF CYLINDRICAL CONFINED JETS

Much attention has been devoted to turbulent incompressible jets. Such flows can be classified as being either free or confined according to their boundary conditions. A jet discharging into an effectively infinite medium is called a free jet. A jet discharging into an enclosure whose solid boundaries have an important influence on the development of the jet, is called a confined jet. The basic difference between a free and a confined jet is that in the free jet the pressure across the jet is essentially constant and the total axial momentum is conserved from one cross section to another, whereas in a confined jet the total mass flow is constant while both the total momentum and the pressure vary axially.

Practically, the ratio of the confinement diameter, D_2, to the jet source diameter, D_1, can be used as a simple criterion to determine which type of flow is to be expected in a particular situation. For $D_2/D_1 > 100$, the flow can generally be considered to be of the free jet type, while in the range $4 < D_2/D_1 < 100$, confined jets exist. Dealy (9) has shown that for $D_2/D_1 = 2$ the flow completely loses its jet characteristics because the flow does not even develop an approximate self-preserving form before the jet reaches the confining wall.

An interesting phenomenon which occurs only in confined jets is that of recirculation or backflow. An eddy of recirculation will exist as a stable part of the flow whenever the jet's capacity for entrainment exceeds the amount of fluid provided by the secondary flow. In other words, such an eddy will exist when the pressure at the mixing tube wall rises enough to reduce the velocity of the ambient fluid to zero. The general flow pattern in the vicinity of such an eddy is shown in Figure 1. Recirculation or back flow is an important factor in mixing devices and in jet flame furnaces.

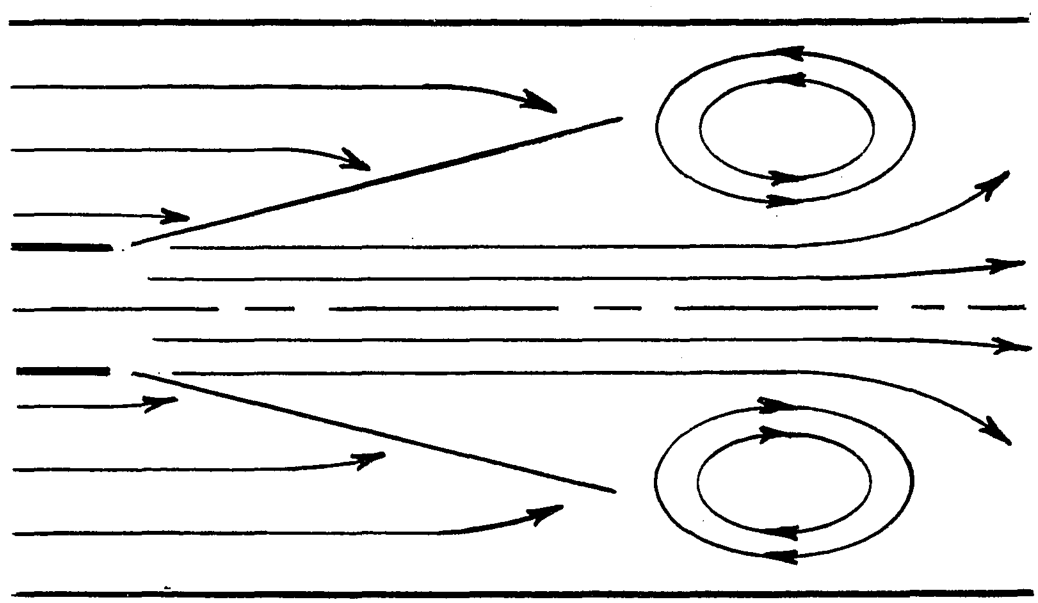

FIGURE 1: RECIRCULATION EDDY

Curtet (6) was one of the first researchers to study confined jets in detail. He was able to develop an approximate theory of confined jets with the following assumptions:

1. Incompressible flow and constant fluid properties
2. Identical fluid properties in both streams
3. Potential flow exists in both streams initially
4. The boundary layer assumptions apply
5. The flow outside the jet is non-turbulent and uniform
6. Wall friction is negligible
7. The mean velocity profiles become similar in form before the jet reaches the mixing tube wall

Curtet found, after integrating the equations of motion across the mixing tube, that the two parameters that appeared in the equation were the ratio R_2/R_1 and a momentum parameter m. This similitude parameter, which expresses in dimensionless form the sum of the momentum flow and the pressure force at a particular cross section, has been found experimentally to be nearly constant from one cross section to another. For a cylindrical confined jet, the initial value of this similitude parameter is :

$$m_o = \frac{R_1^2\,(U_1^2 - U_2^2) + \dfrac{U_2^2\,R_2^2}{2}}{(v_t^2/\pi^2\,R_2^2)} - \frac{1}{2} \qquad (1)$$

With the results of the above theory, Curtet (7) predicted that recirculation in an axisymmetrical confined jet would occur for all values of m_o greater than 1.50 .

In a more recent paper (1), Barchilon and Curtet reported an extensive study of the cylindrical confined jet with backflow. Experiments conducted by these authors have made it possible to characterize the mean structure of the recirculation eddy in terms of the similitude parameter, m_o. A study of the instantaneous structure of the recirculation eddy by photography for $m_o > 11$, revealed that unusually high turbulence levels exist in both the jet and the backflow. The eddy moves back and forth periodically and a group of regular vortices are formed. This observed flow pattern varies considerably with time. The unsteadiness of the flow increases with increasing values of m_o .

Becker (2) has made a more general analysis of confined jet flows. He demonstrated the fundamental significance of the momentum parameter but suggested a new form for the similarity criterion. He called this new parameter the Craya-Curtet number, C_t , defined by :

$$C_t = \frac{1}{\sqrt{m_o}} \qquad (2)$$

For a given ratio of R_2/R_1 , C_t is a unique criterion for dynamic similarity in confined, constant density, fully turbulent jets. Physically, $C_t \to 0$ implies the case of total recirculation and $C_t \to \infty$ means that the flow throughout the confined jet becomes completely uniform. Becker's experiments indicated that recirculation is limited to $C_t < 0.75$.

In the above studies, the ratio R_2/R_1 was greater than ten and the flow from the jet source was uniform and irrotational. Dealy (9) in his studies on confined jets used a fully developed turbulent pipe flow as a jet source and the confinement of the jet was much more severe. His experimental data, however, confirmed the results of both Becker and Curtet. Applying an integral momentum analysis to a very simplified model of the confined jet system, Dealy showed that C_t is the sole parameter that governs recirculation, only if the radial pressure gradient, wall friction and irrotationality in the ambient fluid are negligible and the jet develops a similar form before reaching the confining wall. Quantitatively, the model predicts the onset of recirculation for $C_t = 0.91$ assuming a Gaussian velocity profile and $C_t = 0.83$ for a cosine velocity profile.

Since in the above analysis the shear stress at the wall has been neglected, the predicted maximum pressure recovered is too high, and therefore the predicted critical values of C_t are also too high. Experimentally, this has been confirmed by both Dealy and Becker.

All of the above researchers have confirmed the fact that the effects of jet Reynolds number and detailed structure of the jet, on the recirculation eddy and other features of the flow, are very small as long as the jet Reynolds number is high.

III

A METHOD TO CHARACTERIZE THE MIXING PATTERNS IN A CLOSED VESSEL

A. Introduction

The knowledge of the general flow patterns in heat and mass transfer equipment and chemical reactors is important in their design. Two idealized flow patterns, namely perfect mixing (backmix flow) and plug flow, are of particular interest as limiting cases. A perfectly mixed vessel is one whose contents are spatially uniform in composition at all times. Plug flow through a vessel signifies that there is no mixing at all in the longitudinal direction. Process vessels are often designed to approximate one of these ideal types of flow patterns, since the analysis of the performance of the process vessel is greatly simplified and easily developed if either of the ideal type of flows is approximated.

In general, the mixing that occurs in practical flow systems nearly always lies somewhere between the two extreme mixing patterns. Since this must be taken into account in the proper design of process vessels, it is important to determine the actual flow patterns of the fluid in these vessels.

To obtain the complete flow pattern of the fluid in a vessel by point to point measurements is impractical and often not even possible with existing equipment. A probabilistic treatment is more practical and can be used to obtain some information on the general flow patterns of the fluid in the vessel. This approach requires only the knowledge of the times that different fluid elements reside in a particular vessel. Therefore, in this method, the age of a fluid element is the important parameter.

The general idea of age distribution functions was first introduced by Danckwerts (8). These functions determine only the time that a certain fraction of fluid spends within the vessel (information on macromixing). They do not yield any information about the exact history of the fluid element while inside the vessel (information on micromixing). Both macro- and micromixing information are necessary to completely define the mixing in a particular system. The information on micromixing is difficult to obtain experimentally and is only necessary in equipment where the interaction between fluid elements affects the rate, as for example in chemical reactions of order greater than one. In practice, macromixing information is usually sufficient to take into account the existing mixing patterns in a process vessel in predicting the performance of the vessel. Only in certain cases would micromixing information be absolutely necessary, as for example in a very rapid liquid reaction where the structure of mixing is the most significant aspect (3).

B. Age Distribution Functions

The most important age distribution functions are the internal and exit age distribution functions. The internal age distribution function, $\mathcal{I}$, is defined so that $\mathcal{I}(t)dt$ is the fraction of fluid in a vessel with ages between t and t+dt . Similarly, the exit age distribution function, E , is defined so that E(t)dt is the fraction of fluid in the outlet stream with ages between t and t+dt . The E function thus gives the residence time distribution, RTD, of a fluid in a vessel. For closed vessels, these functions are related by the equation :

$$E(t) = - \tau \frac{d\mathcal{I}(t)}{dt} \tag{3}$$

where τ = mean residence time

$$= \frac{\text{Volume of vessel used by flow}}{\text{Volumetric flow rate through vessel}}$$

$$= \frac{V}{v_t}$$

Thus, the same information can be obtained from either of the age distribution functions, although some aspects of non-ideal flow are often more easily seen in one function than in the other.

Spalding (17) showed that the definition of τ above was valid for steady incompressible flows of arbritary complexity in closed vessels under the following conditions:

1. No diffusion out of the flow system at the inlet and into the flow system at the outlet.
2. No change in specific volume of the fluid as it passes through the system.

The mean residence time can then be related to the E function by the following equation :

$$\bar{t}_E = \int_0^\infty t \; E(t) \; dt = \tau \qquad (4)$$

A check on the validity of the experimentally determined RTD data can be made by comparing the value of τ obtained by equation (4) with the value of τ calculated from its definition.

The E and I distribution functions are usually normalized with respect to the mean residence time by introducing a reduced time variable θ , which is defined by the equation :

$$\theta = \frac{t}{\tau} = \frac{t \; v_t}{V} \qquad (5)$$

When both the dimensionless E and $\mathbf{I}$ functions are plotted against θ , the area under the resulting curves is unity. This is another check on the validity of the experimentally determined RTD data. Figure 2 shows the E and $\mathbf{I}$ functions for the two ideal flow patterns.

Detailed discussions of the above concepts have been given by Levenspiel and Bischoff (14) and by Levenspiel (13).

C. Experimental Methods to Determine the Residence Time Distributions

Residence time distributions are obtained experimentally by a number of techniques, all of which can be classed as stimulus-response techniques. The most common technique is to introduce some tracer material at the inlet of the flow vessel and to measure its concentration in the outflow. Although any type of tracer signal may be used, the most common signals include an instantaneous pulse injection of the tracer, a step change in the tracer concentration at the inlet or a sinusoidal variation of the tracer concentration with time. The latter method is usually used only when the frequency response of the system is being studied, namely in problems of process control.

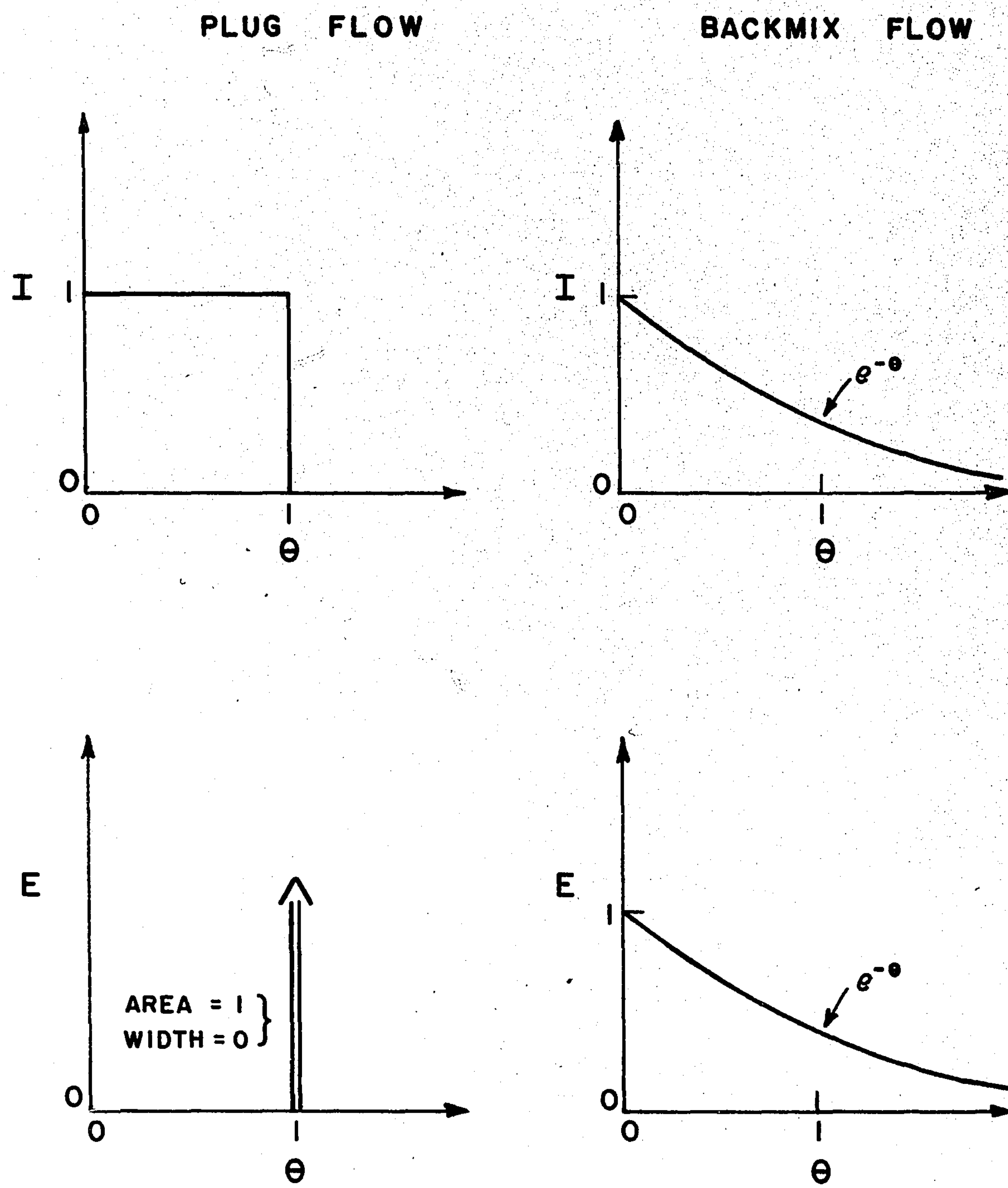

FIGURE 2: PROPERTIES OF THE E AND I CURVES FOR IDEAL FLOW PATTERNS IN CLOSED VESSELS.

If an instantaneous pulse injection is used as an input signal, the outlet tracer concentration, when plotted against time, is called the C curve. If the C curve is normalized so that the total area under the C Curve is unity, it can be shown that the C curve is the same as the E curve.

The instantaneous pulse injection can be represented mathematically by the delta function. The delta function, which is actually a generalized distribution, represents a peak at $t=0$ of infinite height and of infinitesimal width. In practice, this ideal pulse cannot be realized. However, if the time of injection is much smaller than the mean residence time of the material passing through the system, a close approximation of the ideal pulse with respect to the effect on the output response is attainable.

If a step change in tracer concentration at the inlet of the vessel is used as the input signal, the outlet concentration when plotted against time is called the F curve. The dimensionless F function is related to the dimensionless I function by the equation $F + I = 1$. As mentioned earlier, a simple relationship exists between the E and I functions. Hence, the same information can be obtained by either of these experimental techniques.

One of the advantages in using a pulse signal is that the residence time distribution function, E , is obtained directly. If a step signal is used, the E curve can be obtained by differentiating the F curve, but this often leads to large errors. Also, it is often simpler, experimentally, to inject a pulse signal than to create a step change signal.

D. Interpretation of RTD Data

Some information on the fluid flow within a flow vessel can be obtained directly from the E and I functions. If a small degree of mixing is occurring in a vessel, the E function will show only a small amount of spreading, as compared to the E function for ideal plug flow. This situation can be represented with an eddy diffusion or axial dispersion model and the appropriate parameters have been published in the literature (14). However, if the mixing patterns deviate considerably from the ideal flow patterns, the features of dead space, bypassing, and non-uniform regions within the vessel can be introduced to help in the interpretation of the distribution functions.

Dead space is a region in the vessel where the movement of fluid is relatively slow so that this portion of the fluid can be considered to be stagnant. Quantitatively, the fluid which stays in the vessel longer than twice the mean residence time can be considered to be stagnant. However, the cut-off point is arbitrary, depending somewhat on the accuracy of the experimental data. Dead space is indicated on the E curve by a long tail corresponding to the fluid held in the dead space. The same information can be obtained from the $\mathbf{I}$ curve.

If some fluid passes through a vessel at about one fifth or less of the residence time of the main fluid stream, it is said to bypass the vessel. Ideally, for this case, the E curve would have two humps. The first one corresponding to the bypassing fluid and the second one to the main fluid stream. In practice, however, these humps are often smeared and are difficult to distinguish. Bypassing shows up more distinctly on the $\mathbf{I}$ curve, where the initial drop in the $\mathbf{I}$ curve gives a quantitative measure of the amount of fluid bypassing the vessel.

Anything more complex than dead space and bypassing is difficult to determine by visual inspection of the age distribution curves. Some characteristics of the curves, such as moments, have been suggested in order to interpret the RTD data, but these have not proved to be too useful (4). For the case of these non-ideal flow patterns, a flow model is helpful in the interpretation and utilization of the distribution functions. Such models are beneficial for two reasons. First, in order to construct a model, careful consideration must be given to all the physical phenomena occurring within the system, and this may aid in the interpretation of the experimental RTD data. Secondly, the model can be used to predict the effects of varying the parameters of the system and this is important for design purposes.

These flow models consist of a number of interconnected mixing regions such as perfectly mixed, plug flow, dead space, bypassing, and other simple regions. Parameters can be naturally introduced into this type of model, and this makes it suitable for curve-fitting. However, since this model has been derived by a linear process, it can only be applied with certainty to linear processes. A simple illustration will make this clear. A model consisting of a perfectly stirred tank and a plug flow region in series will give the same tracer response curve regardless of which of the two regions comes first. For a linear process, therefore, the calculated output would also be the same for both systems. However, the order of the mixing regions becomes very important for predicting the output of non-linear processes. Thus, unless additional information about the fluid dynamics of the system is available, a model based only on RTD data does not uniquely define that particular flow system. Therefore, for design purposes, it is of paramount importance that the model have a sound physical basis so that it is as much as possible representative of the real system.

Application of mixed models to actual flow vessels have been found to be useful in many systems. Cholette and Cloutier (5) have reported an extensive study on the mixing in a real stirred-tank reactor using such a model. Dixon and Roper (10) have published a report in which a mixed model is used to describe the mixing process in cylindrical tanks with axial inlet and outlet. Levenspiel and Bischoff (14) have applied mixed models to fluidized beds.

IV

LABORATORY STUDIES

A. Introduction

The basic purpose of the experimental program was to obtain residence time distributions in a cylindrical confined jet. This information was obtained by injecting a tracer into the jet flow and monitoring the efflux from the mixing tube. This information could also have been obtained by introducing the tracer into the secondary stream. However, there were two distinct advantages in injecting the tracer into the jet flow. First, it was much simpler experimentally, and second, it was possible to study what happened to the tracer before it entered into the mixing chamber. This would have been extremely difficult to do if the tracer had been introduced into the secondary stream.

There was one piece of information that was not obtainable by injecting the tracer into the jet flow. This was the extent of self-mixing in the secondary stream before it mixed with the jet flow. However, since the secondary stream was non-turbulent, it was assumed that this effect would be negligible.

In this study, concentration was the intensive variable used to obtain the RTD curves; this was simplest experimentally. In practice, electrical conductivity measurements were made to study the changes in concentration of the tracer in the outlet stream. The advantages of this method were twofold. It was possible to receive an almost instantaneous response to changes in tracer concentration with conductivity equipment and the conductance of the efflux could be simply related to the concentration of the efflux. In very dilute solutions, as was the case here, concentration is proportional to the conductance. Mathematically, this is expressed by the equation:

$$C = \frac{1000\ L}{\Lambda_o} \tag{6}$$

where C = concentration in gm-equivalents/liter

L = specific conductance in mhos/cm

Λ_o = equivalent conductance in mhos-cm^2/gm-equivalents at infinite dilution

The tracer used in the experiments was a saturated salt (NaCl) solution. This solution was used because it was more conductive on a volume basis than any other common solution; acids and bases were not considered because of possible damage to the equipment. Also the solubility of the salt solution is a very weak function of temperature, so that the amount of tracer injected would be practically constant for a constant volume setting in the syringe.

B. Apparatus

Figures 3 and 4 show an overall view of the apparatus and a schematic diagram of the experimental equipment respectively. A steady water source was obtained through a centrifugal pump fed by a 45 gallon constant-head tank. The flow rates were regulated by a needle valve in the jet flow line and a globe valve in the secondary flow line. The flow rates in both jet and secondary streams were measured with rotameters. The flow conditioning and mixing chambers were made of 1/4" thick plexiglass. At the exit from the mixing tube, all the fluid passed through the conductivity probe and then out to the drain. The output from the conductivity probe was continuously monitored and recorded.

The secondary flow entrance section is shown photographically and schematically in Figures 5 and 6 respectively. The secondary stream entered the 4" I.D. section through two diametrically opposed ports, each 3/4" in diameter. The flow then passed through a baffle, perforated with a dozen 1/2" diameter symmetrically spaced holes, which reduced the size of the eddies. Any turbulence

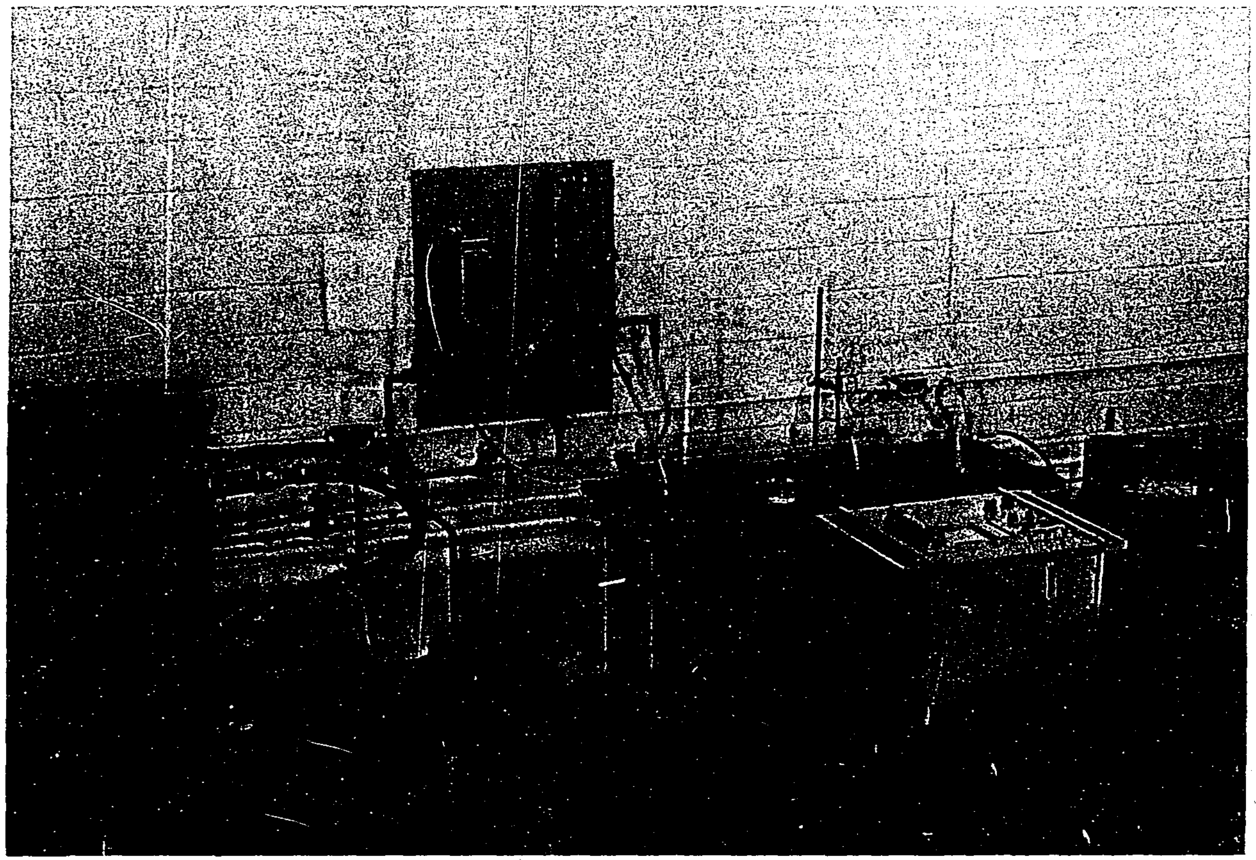

FIGURE 3 : OVERALL VIEW OF THE APPARATUS

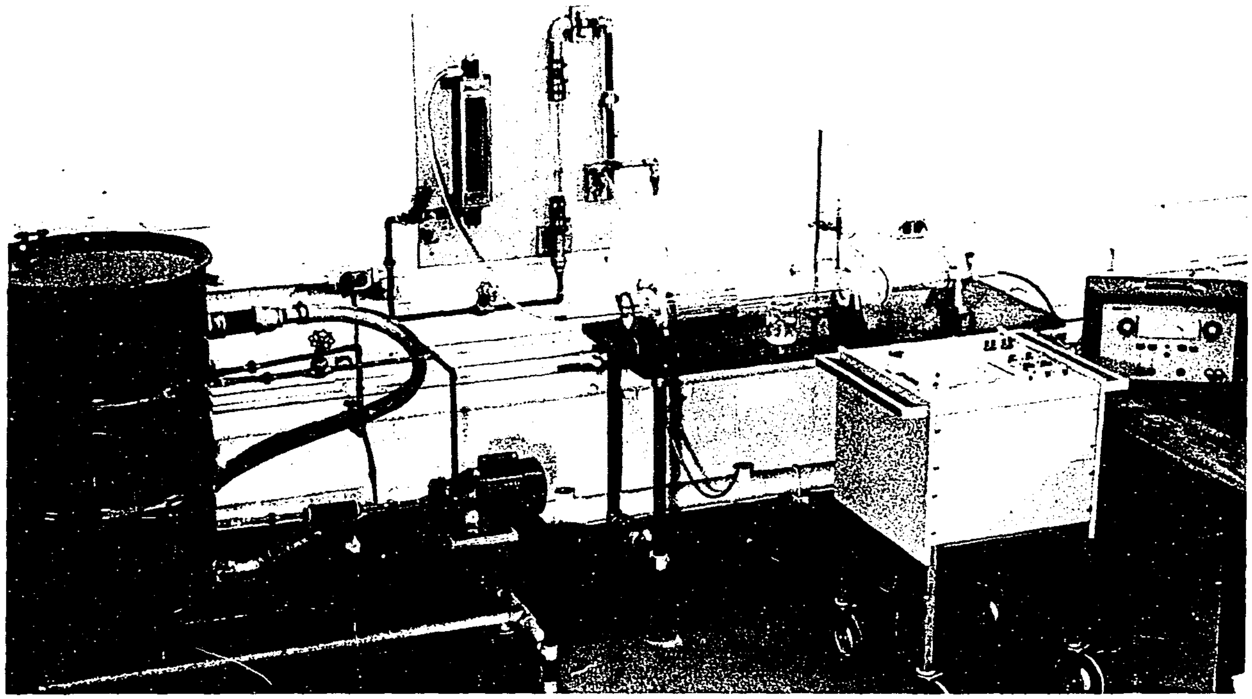

FIGURE 3 : OVERALL VIEW OF THE APPARATUS

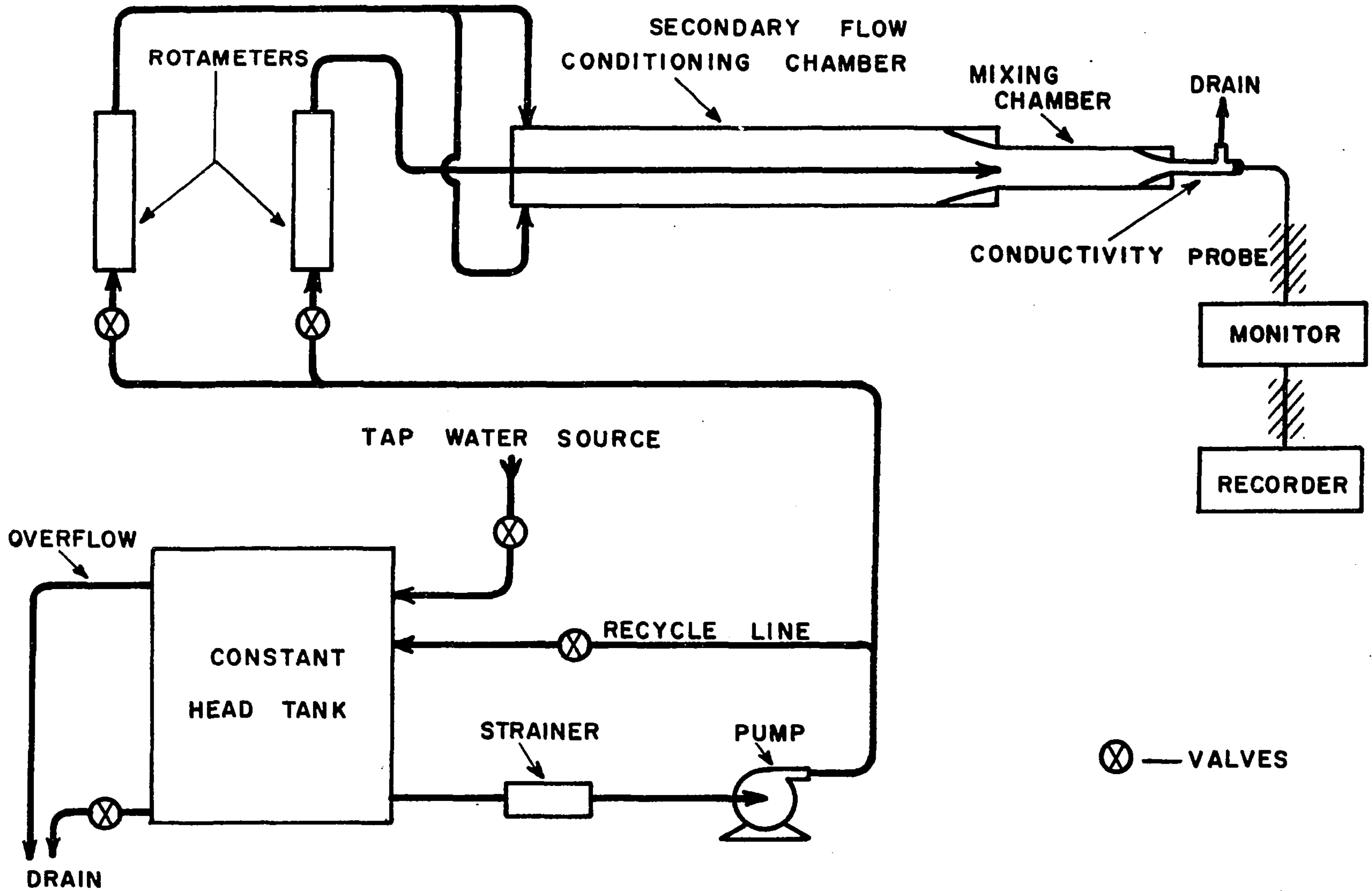

FIGURE 4 : SCHEMATIC DIAGRAM OF THE EXPERIMENTAL EQUIPMENT

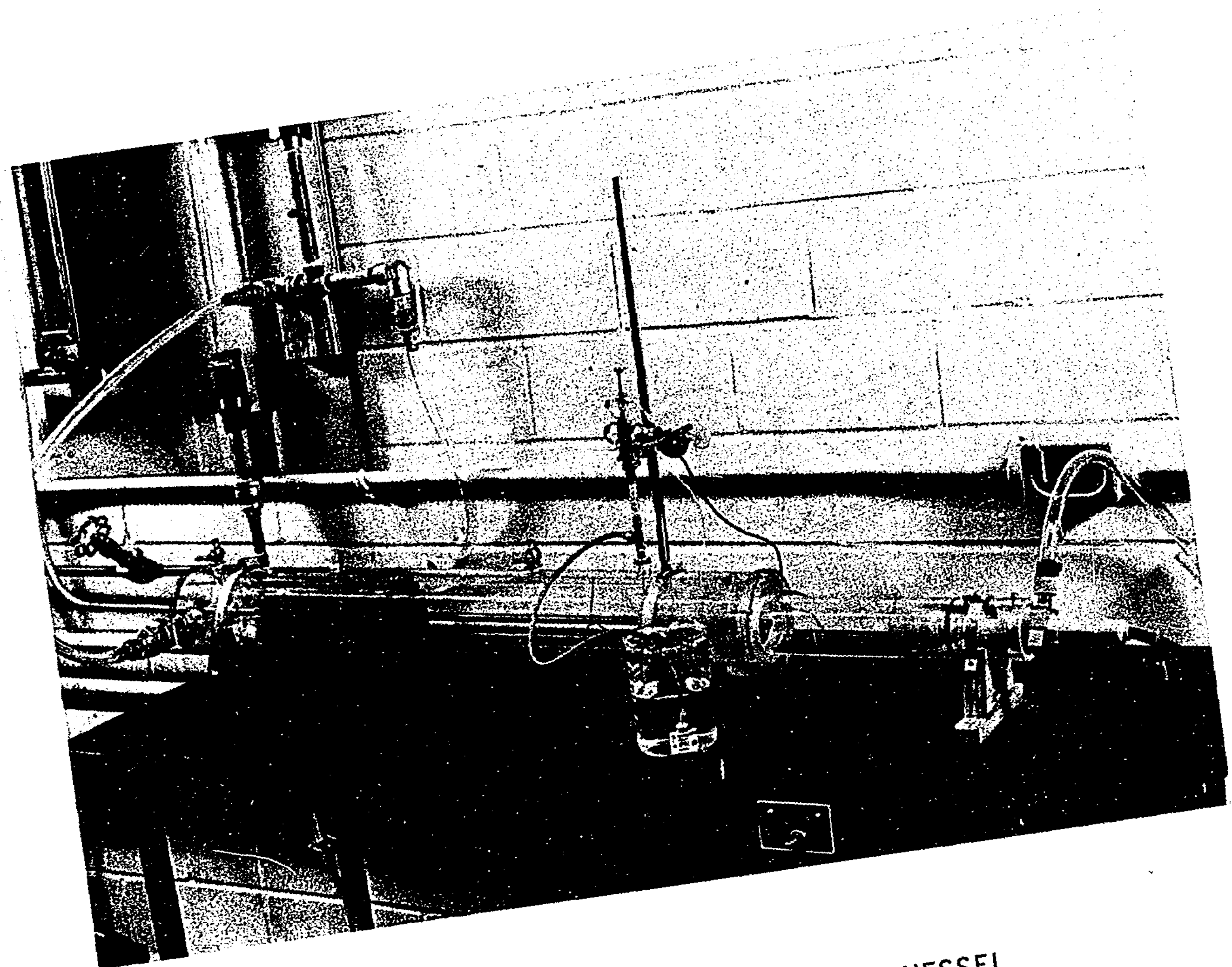

FIGURE 5 : CLOSE-UP OF THE FLOW VESSEL

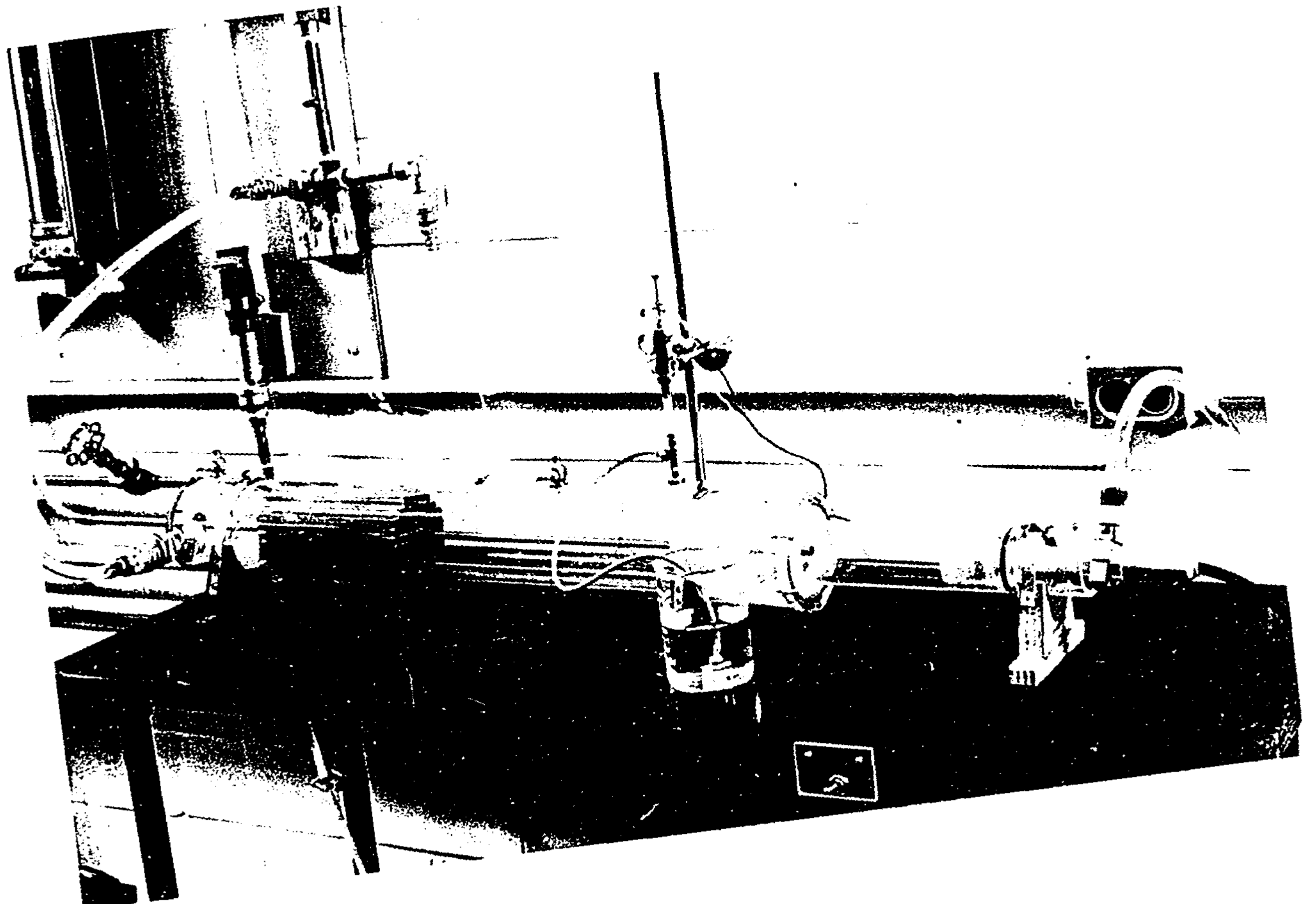

FIGURE 5 : CLOSE-UP OF THE FLOW VESSEL

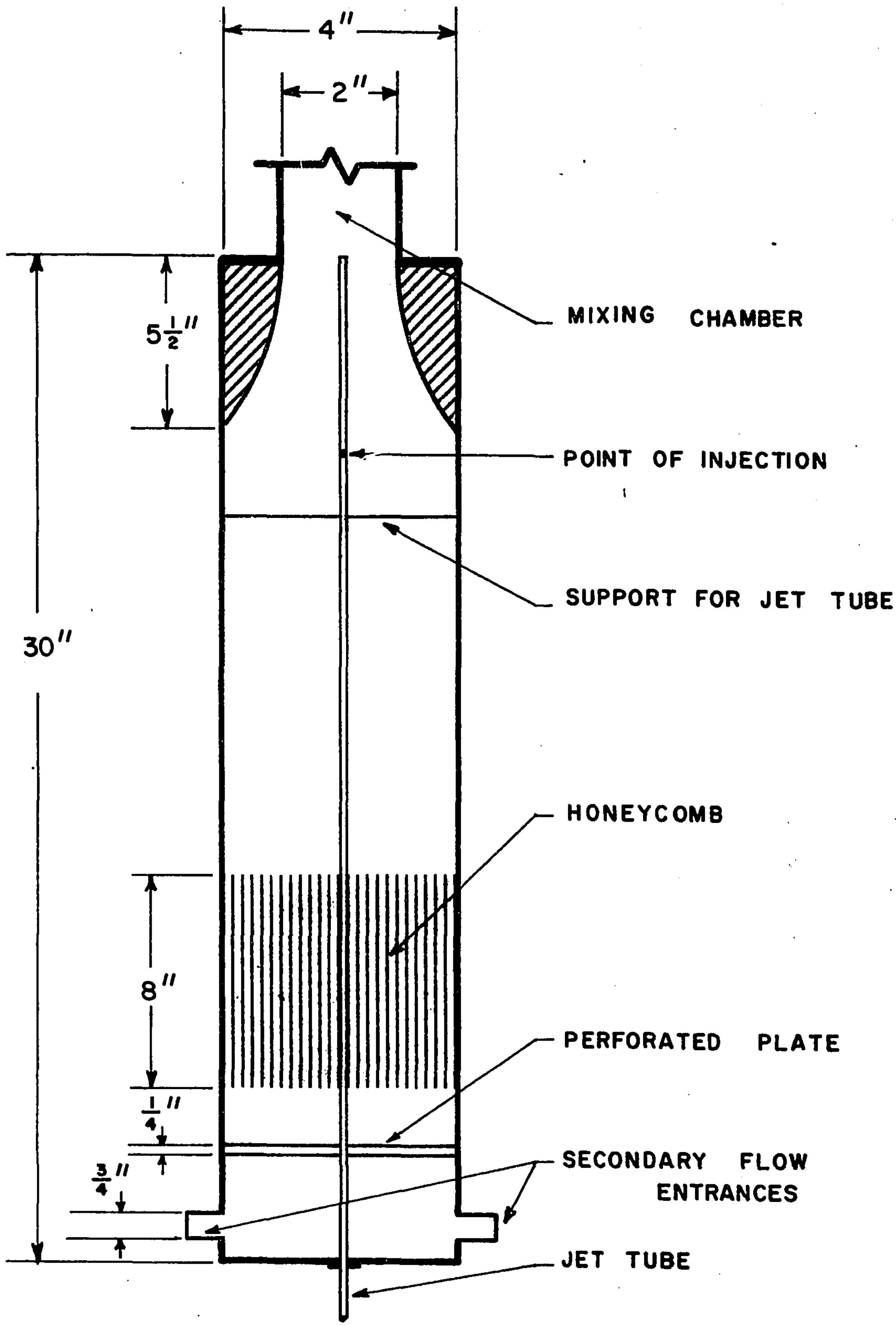

FIGURE 6 : SECONDARY FLOW CONDITIONING CHAMBER (Not to scale)

in the flow was damped out as the stream passed through a 3/8" diameter honeycomb section 8" long and a further calming section 14" long. The flow then entered a converging section 5" long, where the inside diameter was decreased from 4" to 2". The purpose of this section was to produce a uniform velocity profile in the secondary stream as it entered the mixing chamber. A uniform velocity profile and a condition of non-turbulence in the secondary stream as it entered the mixing chamber were necessary so that the experimental conditions would be in agreement with the boundary conditions used in the theoretical analysis of the cylindrical confined jet.

The jet source was a thin-walled stainless steel tube with an I.D. of 0.355". The jet tube was supported by the baffle, the honeycomb section and a ring held in position by three thin rods situated at 8" from the entrance of the mixing chamber. The length of the jet tube was greater than 100 jet tube radii, to insure a fully turbulent pipe flow jet source.

The mixing chamber is schematically shown in detail, in Figure 7. This section had a 2" I.D. and its volume was adjustable. The flow from the mixing tube passed into a converging section whose axial position could be adjusted, then through the conductivity probe and out to the drain

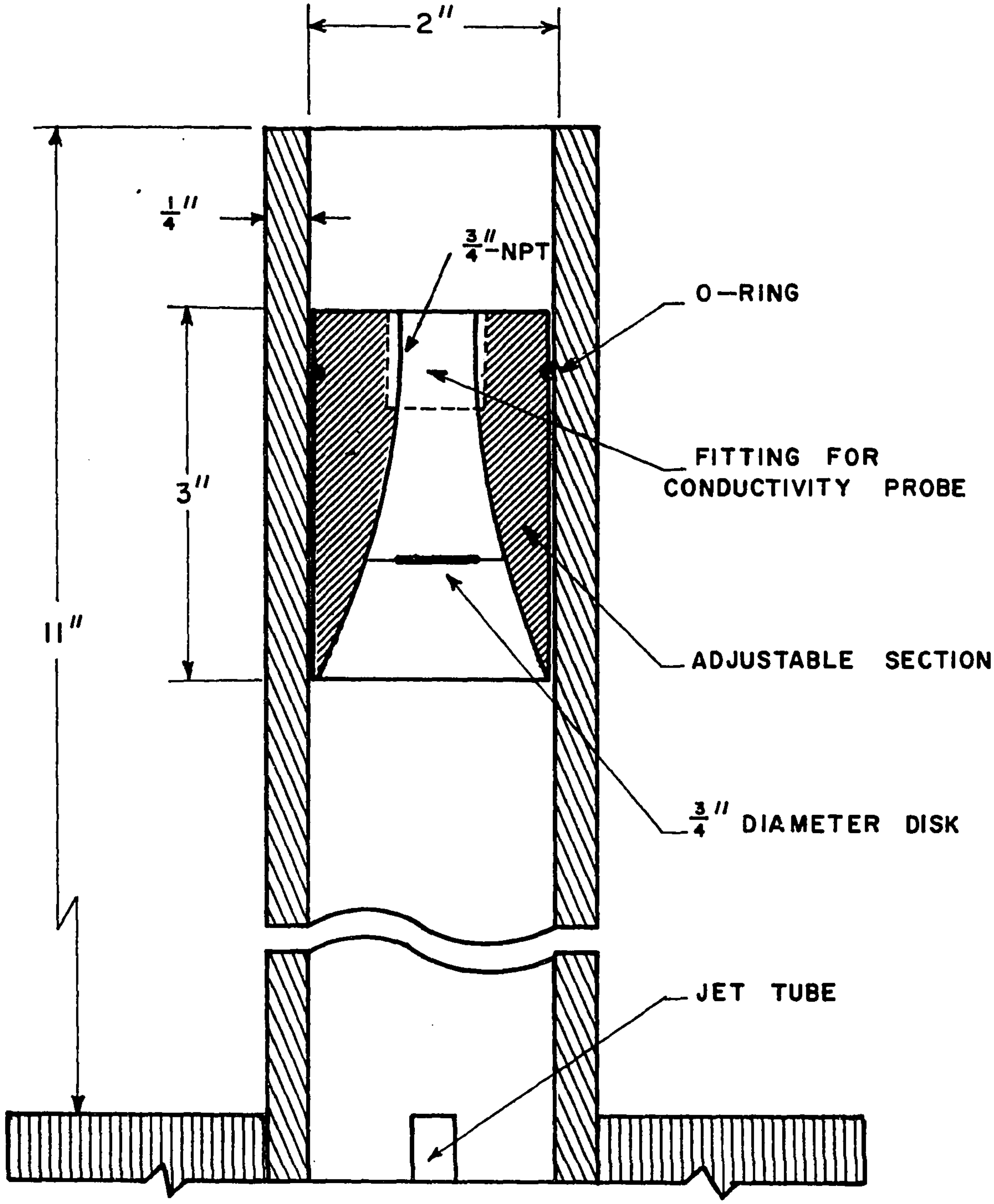

FIGURE 7 : MIXING CHAMBER (Not to scale)

through 1/2" I.D. tygon tubing. The 3/4" diameter disk in the converging section was added to promote radial mixing. Since only axial mixing was of interest, it was desirable to measure the radially mixed average concentration of tracer material in the outlet stream.

A photograph of the injection system is shown in Figure 8. The tracer injector was a B-D Cornwall continuous pipetting outfit graduated in 0.02 cc. The syringe was connected to a no. 16 syringe needle through a luer-lok fitting. The needle was soldered onto the surface of the jet tube 6" from the entrance of the mixing chamber. The location of the needle was determined by two basic requirements. First, the point of injection had to be as close as possible to the entrance of the mixing chamber so that a minimal amount of tracer diffusion would take place in the jet tube. Second, the needle had to be far enough away from this entrance so that it would not disturb the flow in the secondary stream.

The instruments used to obtain the tracer concentration in the outlet stream were as follows. The resistance of the flow in the outlet stream was measured by a Leeds and Northrup conductivity probe (flow-through-type assembly no. 4803), with a cell constant of 10; see Figure 9. The signal as received by this probe was monitored by a Wayne

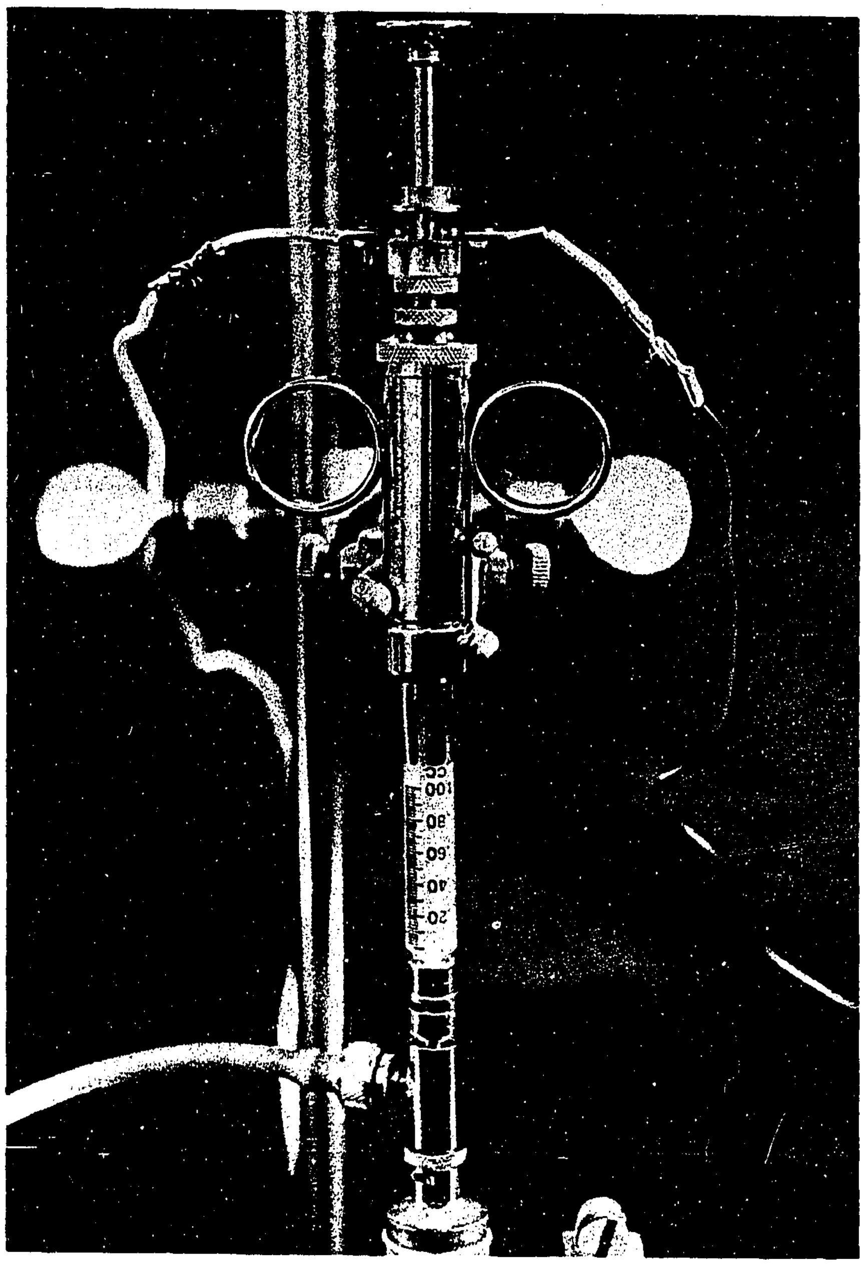

FIGURE 8 : THE INJECTION SYSTEM

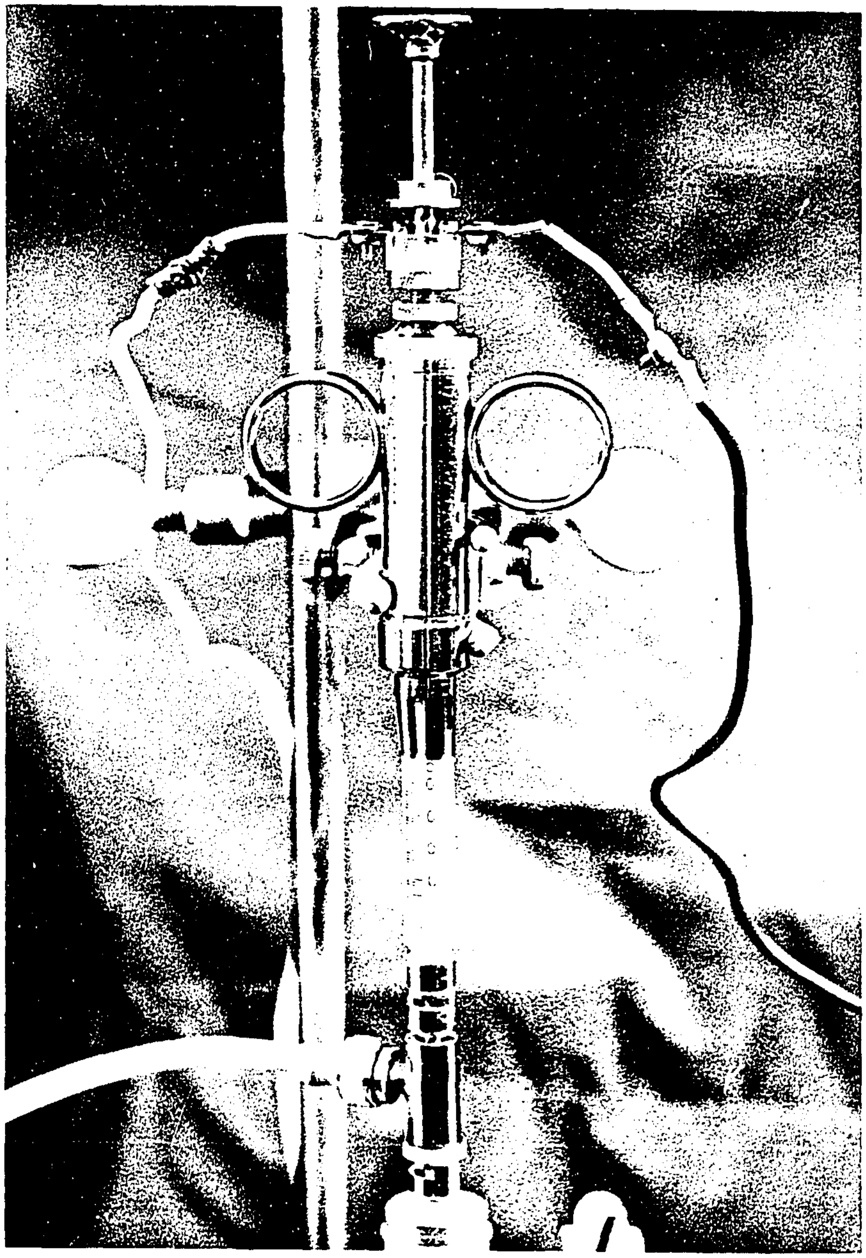

FIGURE 8 : THE INJECTION SYSTEM

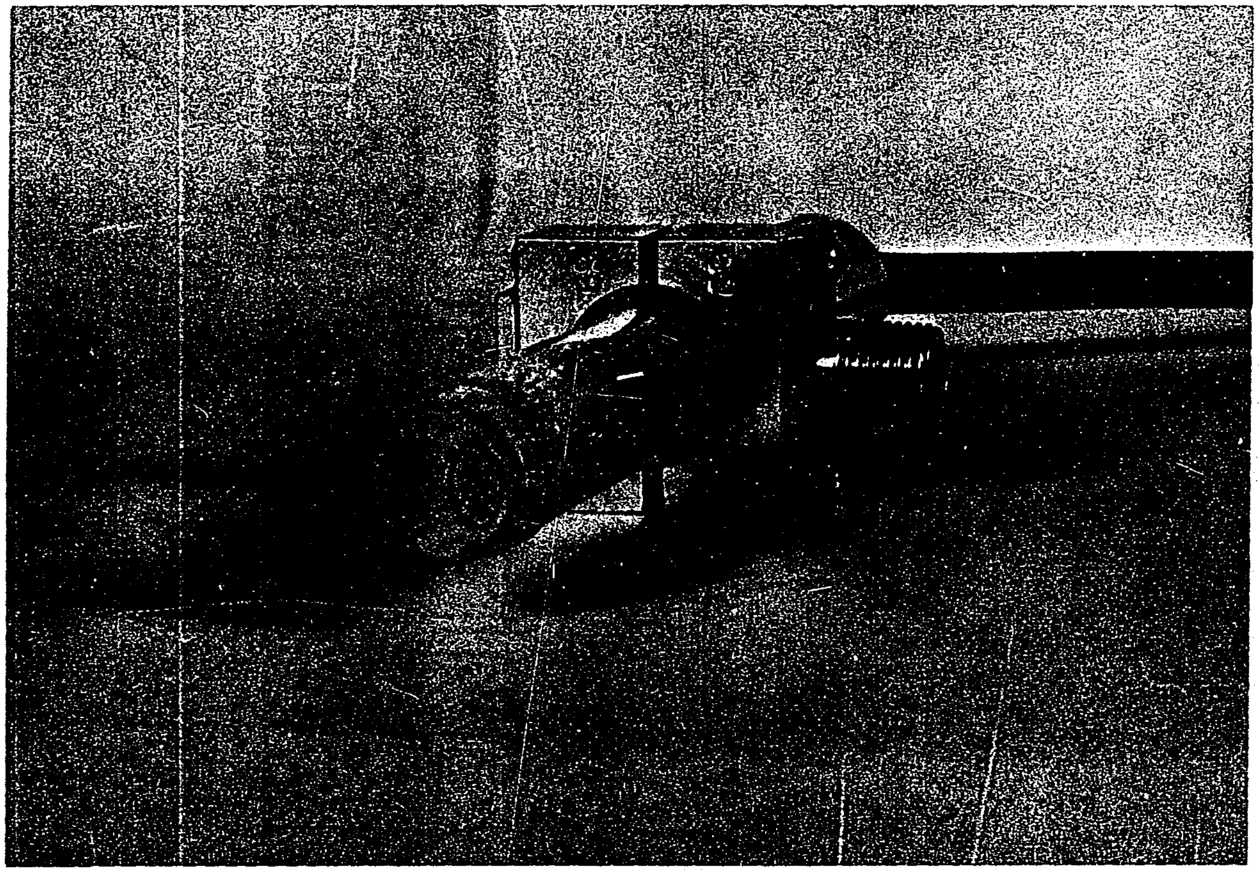

FIGURE 9 : THE CONDUCTIVITY PROBE

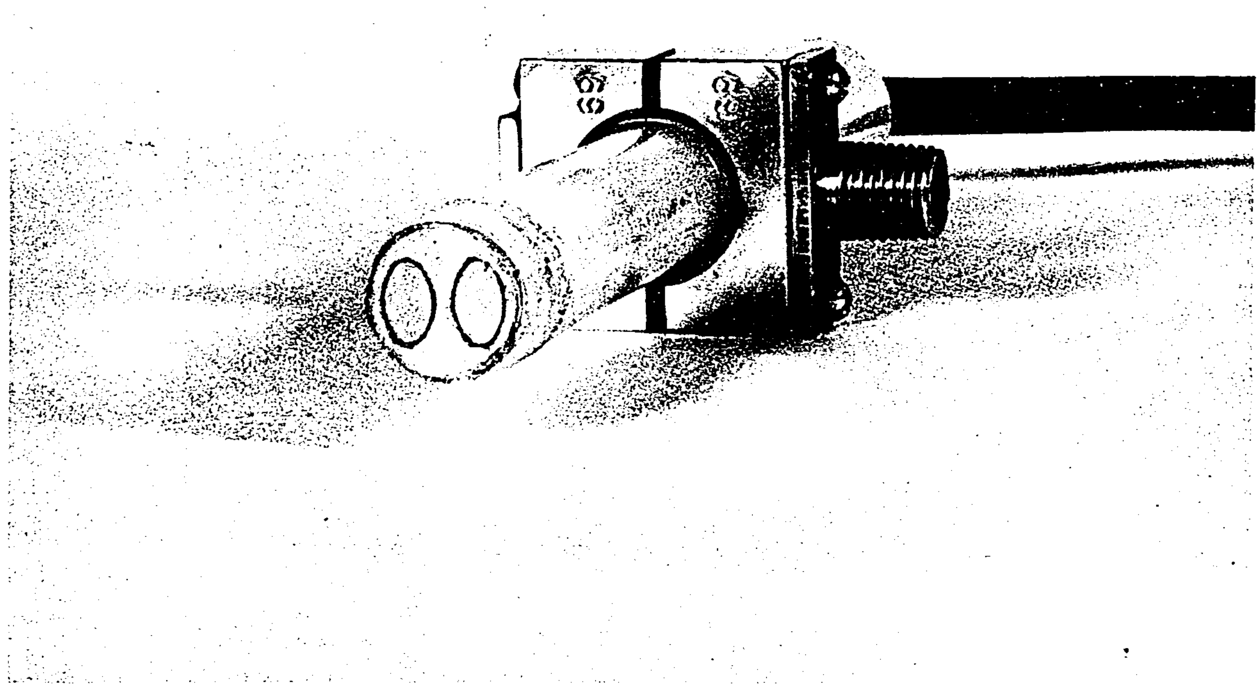

FIGURE 9 : THE CONDUCTIVITY PROBE

Kerr autobalance conductance bridge, model no. B5416. This instrument gave the conductance in mhos. The output from the conductance bridge was recorded on a high speed Sanborn recorder. The injection system included a switch that closed an electric circuit powered by a 1.5 volt dry cell when the plunger in the syringe reached its end position, as shown in Figure 8. The signal that resulted was recorded on the second channel of the recorder. The point when this signal first increased from zero was designated by t' . This point was important in the determination of t_o $(t=0)$ for this system, as will be shown in the next chapter.

C. Preliminary Studies

The secondary flow conditioning chamber was designed to produce a uniform velocity profile at the entrance to the mixing chamber. To check the success of this design, the velocity profile was measured at the entrance of the mixing chamber across a horizontal diameter. A simple pitot tube arrangement with the wall pressure as the reference pressure was used. Because the pressure differences were expected to be less than 0.2 mm of Hg, a very sensitive pressure transducer MKS Baratron pressure meter, type 77, was used. Since this instrument can be used directly for gases only, the pressures from the pitot tube and the wall were transferred to air through thin impermeable membranes. The height of these membrances above an arbitrary datum plane was adjusted to be exactly the same using a cathetometer. This was necessary so that the hydrostatic head in the liquid lines cancelled each other. The results indicated a nearly uniform velocity profile.

A material balance was conducted on the tracer material to check the accuracy of the measuring technique. Since the material injections were not exactly reproducible for a fixed syringe setting, an averaging method was employed. The amount of tracer input was determined by injecting ten consecutive shots of tracer solution into a weighed beaker, evaporating the water and weighing the remains. The amount of tracer output was determined by injecting ten consecutive injections of tracer solution into the confined jet system, to produce ten concentration versus time curves. From these, it was possible to calculate the amount of tracer output, as shown in Appendix 1. The material balance was conducted for both high and low flow rates.

In the calculations to determine the tracer output, the equivalent conductance at infinite dilution was used. However, the average concentration of the tracer output curves was such that this assumption of infinite dilution was not strictly valid. Corrections for this effect increased the apparent amount of tracer recovered by about 1.5 %.

When the first material balance was made with injections of 0.3 cc. of saturated salt solution, apparent recoveries were found to be only about 80 % or less. This was thought to be due to imperfect radial mixing in the outlet stream. To increase the radial mixing, a 1/2" diameter disk was installed in the converging section just before the conductivity probe. The measured recoveries were then in the range of 85 % - 95 %, depending on the total flow rate. With a 3/4" diameter disk, measured recoveries were about 98 % or better for all flow rates. All reported data were taken with the 3/4" diameter disk installed.

During the experimental runs that were made to check the material balance, considerable fluctuations were noticed in the tracer output curves under identical flow conditions. These fluctuations were present in flows with and without recirculation. It appeared possible that there might have been some periodicity in the flow. To check this hypothesis, a constant rate injection experiment was carried out. Tracer concentration output curves were obtained for flows with $C_t = 1.009$ and 0.695. The output tracer curves using constant rate injection showed that the greater the injection rate of tracer solution, the greater the fluctuations in the tracer output curves. However, for low injection rates, an almost steady concentration of tracer was obtained in the outflow. It was concluded that the fluctuations in the output curves were mainly caused by the tracer injection technique.

In order to eliminate, or at least sufficiently decrease the undesirable effect mentioned above, smaller injection samples were tried. It was found that the smallest tracer pulse that could be injected to give a reasonably sized tracer output curve was about 0.09 cc. The result of using these smaller injection samples was to nearly eliminate the fluctuations in the output curves and to reduce the injection time. The latter effect was important since an ideal pulse was to be approximated.

Another experiment was carried out to study the tracer impulses in the jet tube. The purpose of this study was twofold; to observe the shape of the injected pulses as they entered the mixing chamber, and to find t_o for the system. The experimental layout is depicted in Figure 10. The mixing chamber was removed and a small plexiglass section was added to fit over the jet source. The results of this study are discussed in detail in the following chapters.

D. Procedure

The experimental program was designed so that RTD data would be obtained for both recirculatory and non-recirculatory flows. Thus, data were collected in the range of Craya-Curtet numbers from about 0.5 to 1.0. The fact that the

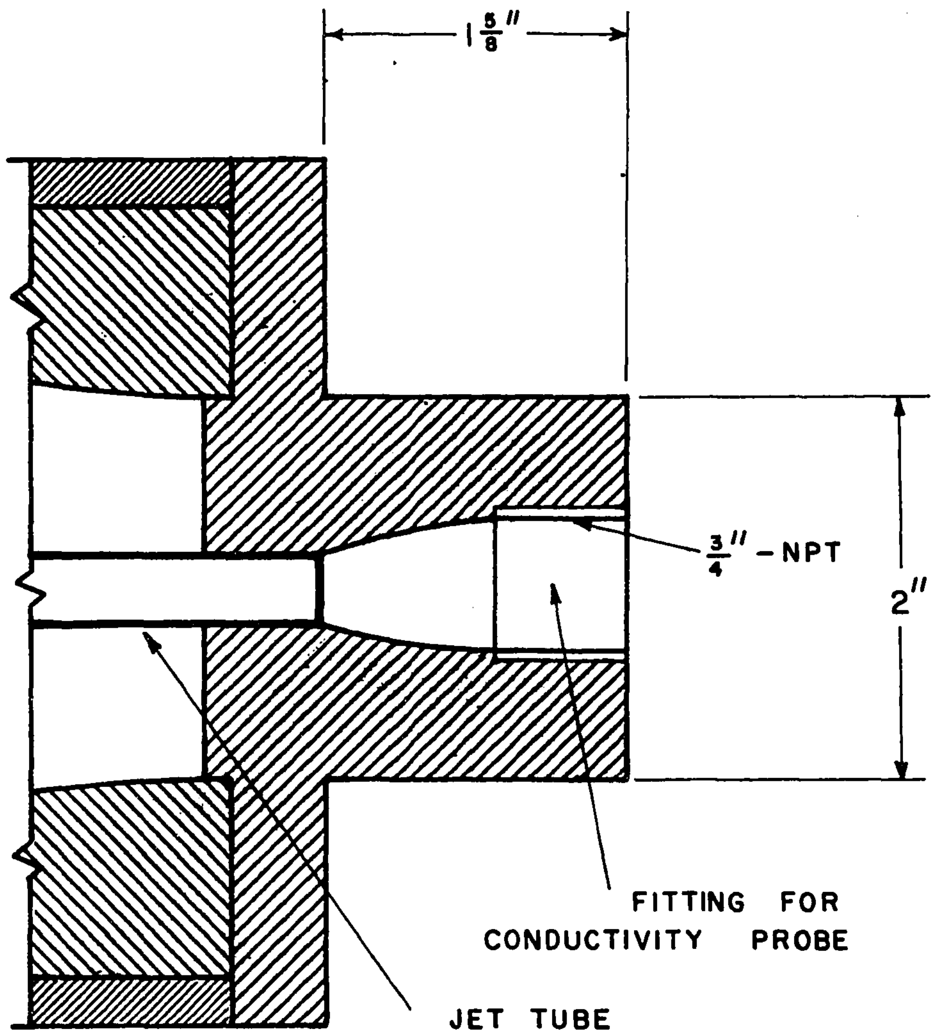

FIGURE 10: APPARATUS TO STUDY THE PULSE INJECTIONS AT THE END OF THE JET TUBE.

jet Reynolds number has little effect on the recirculation phenomenon has already been mentioned. Hence, all the data in this study were taken at jet Reynolds numbers of around 4500. Deviations in the Reynolds number were due to changes in the tap water temperature, since the volumetric flow rate in the jet tube was fixed. Variations in the Craya-Curtet number were achieved by varying the secondary flow rate.

The axially adjustable converging section in the mixing chamber was placed so that for the highest secondary flow rate used, the jet spread to the mixing tube wall before entering this section. This position was found by visual observation of injected coloured dye in the jet flow. If the mixing volume had been smaller than this, the converging section would have probably interfered with the jet's development. If it had been much larger, one would have been studying not only the mixing in the developing jet region, but also the effect of downstream pipe mixing. The actual mixing chamber volume, as measured from the jet source, was about 425 cc. Some data were collected with the mixing volume decreased by 15 %, to see what effect this would have on the RTD curves of the system.

For an actual run, the instruments were allowed to warm up and the feeding tank was filled. The flow rates were adjusted and the water flowed through the system until the tap water temperature became quite constant. Air was removed from the flow conditioning and mixing chambers by raising the table on which the apparatus was fixed at one end and allowing the air to escape through air vents in the flow conditioning chamber. A few trial injections were made to fill the injection needle. The recorder was zeroed with plain tap water flowing. Then, the chart of the recorder was turned on to the 100 mm/sec paper speed and the actual recording of data began. Just enough time was allowed between injections so that the needle of the recorder returned to the zero line, before the next pulse was injected. This was to minimize any diffusion of tracer solution that might have taken place from within the needle to the jet flow. After three or four dozen injections had been made, the secondary flow rate was changed, and the procedure was repeated.

V

EXPERIMENTAL RESULTS

A. Data Reduction

Under identical flow conditions, the output tracer concentration curves for different runs varied widely, especially with regard to maxima in the curves. Curves with one, two and sometimes three distinct peaks were found for both recirculatory and non-recirculatory flows, as can be seen in Figures 11 and 12. Such variation in the shape of the output curves must have been related to inconsistencies in tracer injections, since the data were taken under identical flow conditions; i.e., differences in the number of maxima of the output curves were due to differences in the input pulses. This conjecture was confirmed by the results of the study of the tracer pulses at the end of the jet tube, where pulses with more than one peak were found, as shown in Figure 13. Moreover, the majority of these curves had double peaks.

At low values of C_t, where a large portion of the fluid is being recirculated, there is some unsteadiness in the flow. However, this was thought not to be sufficient to cause several distinct peaks in the output curves, because fluctuations in the tails of these curves were never very great.

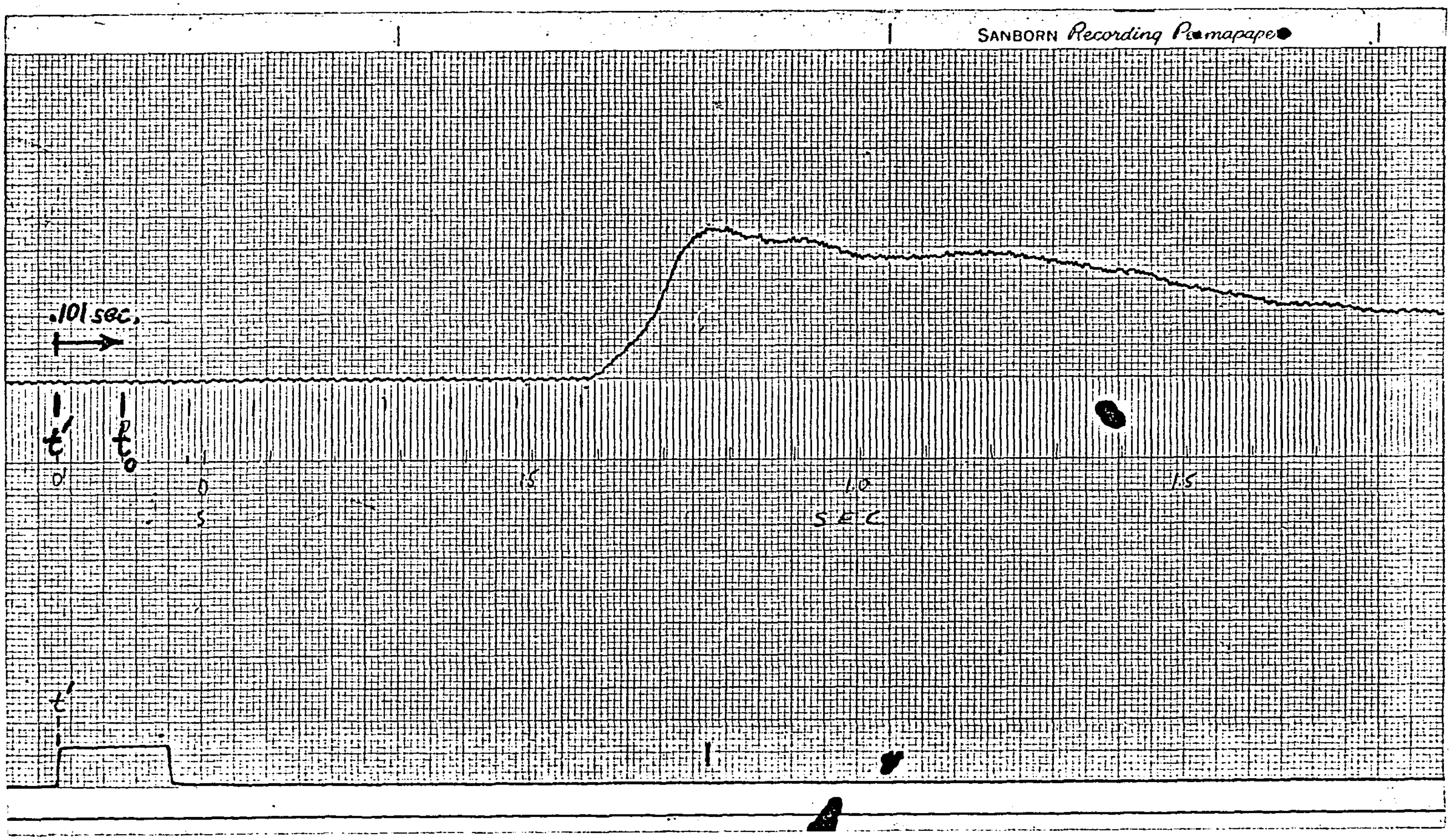

FIGURE 11 : RECORDER TRACE OF CONDUCTIVITY SHOWING THE PROCEDURE TO FIND t_o
($C_t = 0.577$)

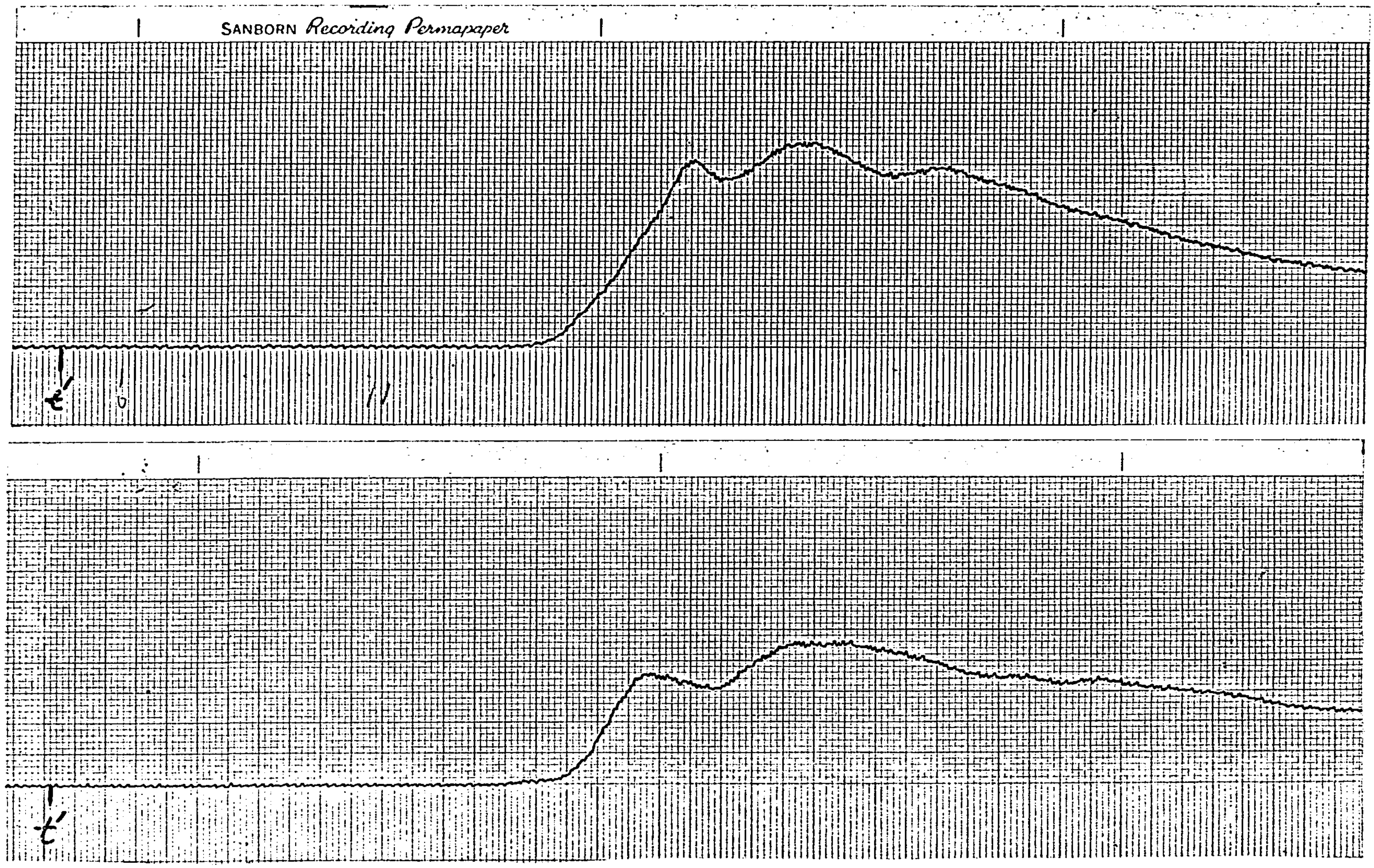

FIGURE 12 : RECORDER TRACE OF CONDUCTIVITY SHOWING MULTIPLE PEAKS ($C_t = 0.577$)

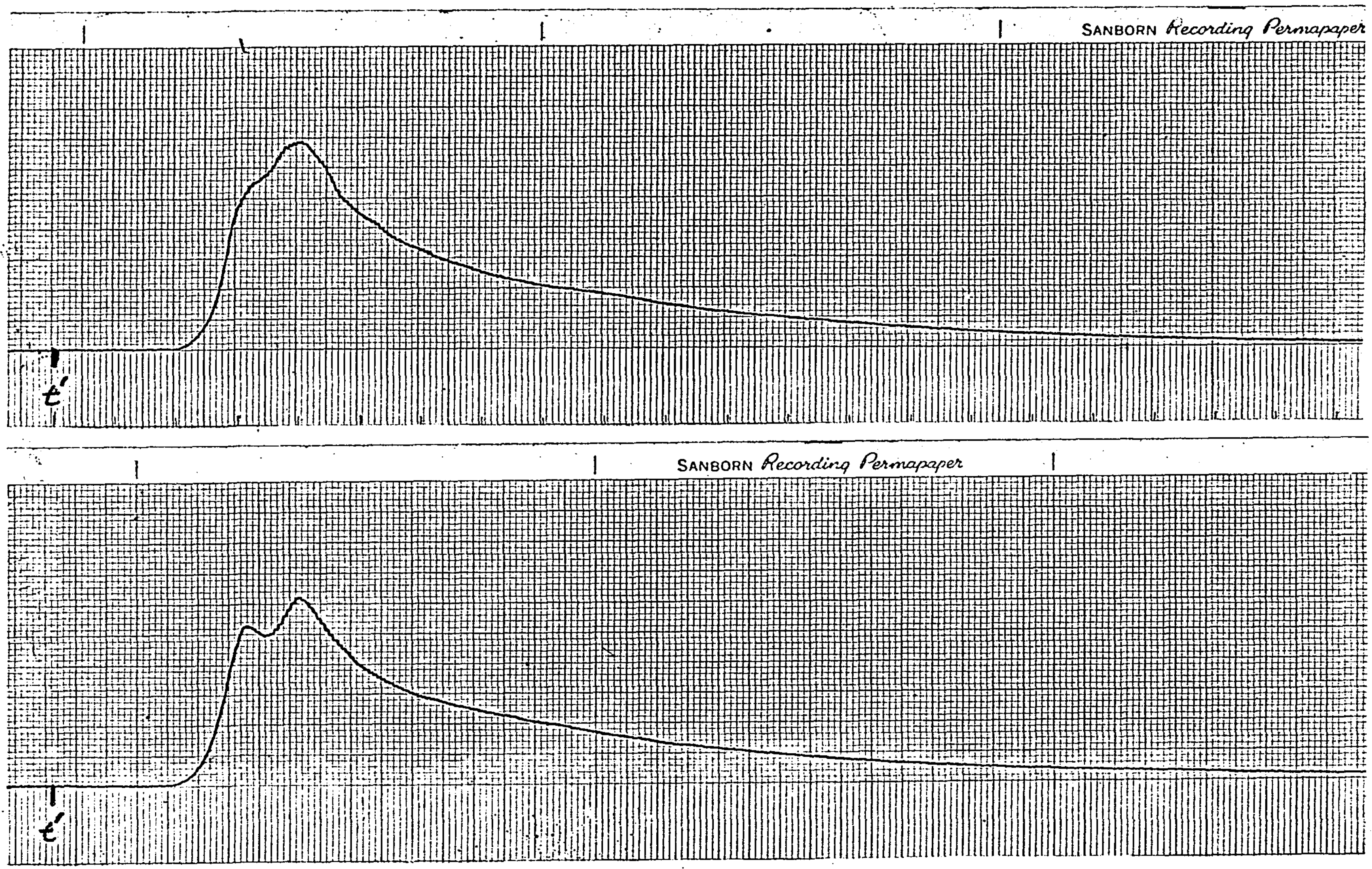

FIGURE 13 : RECORDER TRACE OF CONDUCTIVITY MEASURED AT THE OUTLET OF THE JET TUBE FOR A FIXED REYNOLDS NUMBER

It was concluded that the shape of the output curves, especially in the vicinity of the peaks, depended on the injection technique, which was subject to uncontrolled variation. The data could not, therefore, be subjected to a meaningful statistical analysis. The criteria used in deciding which curves best represented the impulse-response residence time distribution of the fluid in the confined jet system are discussed in the following paragraphs.

Ideally, the pulse injection curve should be in the form of a delta function. This was physically impossible. If the injection time were very much smaller than the mean residence time, however, the pulse created would be practically ideal. In this study, an attempt was made to minimize the ratio of injection time to mean residence time. It is felt that the tracer concentration curves that resulted were representative of the actual residence time distribution of the fluid in this system. Also, a signal similar to that actually used can be easily simulated on a computer for modelling purposes. Thus the basic criterion in choosing curves for analysis was that these curves were to have resulted from pulse injections that minimized the ratio of injection time to mean residence time.

As a first step in data reduction then, curves with more than one distinct peak were disregarded. However, there remained the problem of screening the remaining data curves. To aid in this elimination process, an analog circuit was set up to solve the continuity equation for a perfectly stirred tank with square pulse inputs. This problem can be solved analytically but the analog computer conveniently gives the output curves directly in graphical form. The results of this investigation showed that the concentration in the outlet stream rises linearly for the duration of the pulse and then declines exponentially in the usual fashion for perfectly stirred tanks. The angle of rise is a function of both the amount of tracer introduced into the tank and the duration of the input signal.

Of course, the system under study was far from being a perfectly stirred tank, but some of the analog observations helped to interpret certain features of the experimental curves. Thus it was inferred that curves in which the tracer outlet concentration rose at the fastest rate to the peak concentration in the shortest time resulted from pulses closest in form to the delta function. Suitable curves were selected on this basis.

A considerable change of slope in the rising concentration curve suggested large deviations from the square pulse input signal. Such curves were not analyzed.

If several curves remained after the above criteria had been applied, then the curve corresponding to the injection of the smallest amount of tracer material was chosen. By choosing this curve, problems resulting from inconsistent input pulses were minimized.

It should be emphasized that this was not a process of discarding spurious data. It was simply a process of selecting those data which lent themselves best to direct analysis without detailed knowledge of the stimulus pulses.

B. Data Analysis and Presentation

The zero time, t_o, for this system is defined as the time at which tracer material first enters the mixing chamber. This time was found by analyzing the output curves that were obtained in the study of the injection pulses at the end of the jet tube. The procedure for determining this time for experiments at a fixed Reynolds number is described below.

The injection system was constructed so that when the plunger in the syringe reached its end position, indicating the completion of an injection, a signal was registered on the recorder. The point at which this signal was first registered, was designated by t'. The time interval between t' and the point where the outlet tracer concentration first rose from zero was measured on the recorder output curves. For twenty consecutive injections, this time had an average value of 0.195 seconds with a mean standard deviation of 1.61%. Assuming plug flow in the jet tube, the time the first quantity of tracer entered the mixing chamber was then found by multiplying the above time by the ratio of the volume of the jet tube to the volume of the entire system under study. This calculation gave a time of 0.101 seconds. Thus, for any tracer output curve of the confined jet system, at the fixed jet Reynolds number, t_o was found by adding 0.101 seconds to t'. This procedure is illustrated in Figure 11.

The time interval between the moment the first quantity of tracer material entered the mixing chamber and the moment the tracer material first contacted the electrodes of the conductivity probe was called t*. This time delay is indicative of a plug flow element in the mixing system; higher values of t* corresponding to smaller effective plug flow volumes. This is easier seen by dedimensionalizing t* with τ, calling the resulting function θ*. Values of θ* decrease with decreasing values of C_t, indicating a decrease in the plug flow element in the mixing system. Values of t* for different values of C_t were calculated by a statistical procedure. The results of this analysis

C_t	Number of Curves Analysed	t*	Mean Standard Deviation
		sec	%
.510	32	.740	2.95
.577	40	.700	3.11
.631	50	.676	2.95
.695	35	.654	2.61
.754	40	.639	2.85
.815	40	.623	2.55
.875	40	.612	2.44
.942	30	.595	2.77
1.009	30	.582	2.55
1.078	30	.567	1.85

TABLE 1: EXPERIMENTAL RESULTS FOR THE TIME DELAY t*

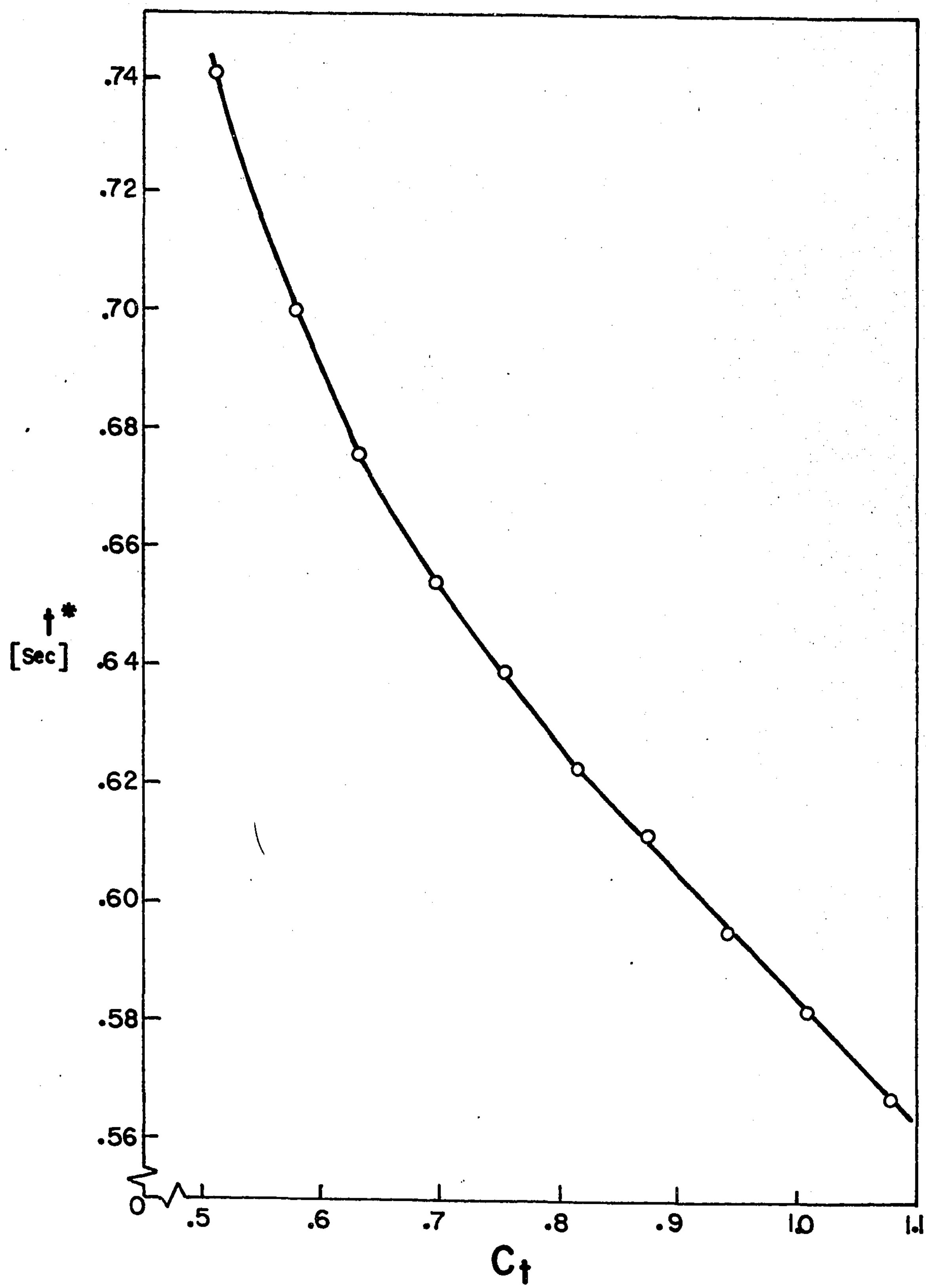

FIGURE 14: EFFECT OF THE CRAYA - CURTET NUMBER ON THE APPARENT PLUG FLOW RESIDENCE TIME

are shown in Table 1. The curve of t^* as a function of C_t is shown in Figure 14. The equations representing this curve were found by a least square analysis. They are :

$$t^* = 0.798 - 0.214\ C_t \qquad 0.80 < C_t < 1.10 \qquad (7)$$

$$t^* = e^{-0.594\ C_t} \qquad 0.50 < C_t < 0.76 \qquad (8)$$

The data fitted equations (7) and (8) with a mean standard deviation of 0.08% and 1.59% respectively.

The tail part of a tracer output curve was found to have an exponential shape. The initial slope of the exponential, called S, was obtained by plotting the tail of an output curve directly on semi-logarithmic paper. The slope, S, had units of $(\mathrm{sec})^{-1}$. This exponential decay curve is exactly what one would obtain from a perfectly stirred vessel having a mean residence time equal to the reciprocal of the slope S. Thus, the smaller the value of S, the greater the volume of a corresponding "perfectly mixed region". Values of S were determined by a statistical procedure. The results are given in Table 2. A curve of S as a function of C_t is shown in Figure 15. The equations for the lines were found by a least square analysis. These are:

$$S = -0.39 + 2.51\ C_t \qquad 0.80 < C_t < 1.10 \qquad (9)$$

C_t	Number of Curves Analysed	S	Mean Standard Deviation
		$(sec)^{-1}$	%
.510	4	.788	0.64
.577	8	.950	4.10
.631	10	1.120	5.28
.695	10	1.292	3.01
.754	8	1.444	3.83
.815	7	1.656	2.93
.875	10	1.814	3.88
.942	10	1.973	2.76
1.009	8	2.141	2.84
1.078	7	2.322	4.08

TABLE 2: EXPERIMENTAL RESULTS FOR THE EXPONENTIAL SLOPE S

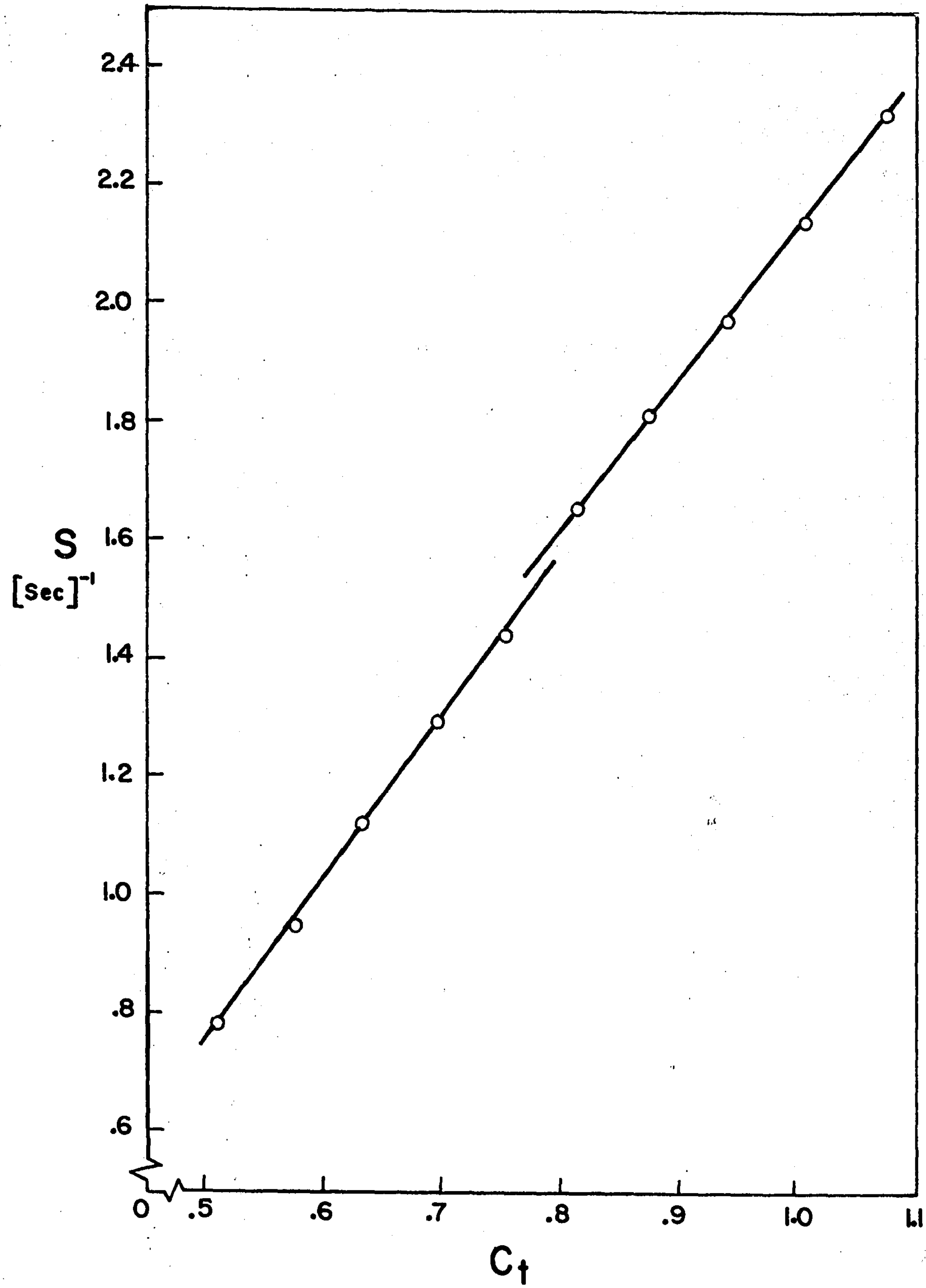

FIGURE 15 : EFFECT OF THE CRAYA - CURTET NUMBER ON THE APPARENT PERFECT MIXING RESIDENCE TIME

$$S = -0.61 + 2.73\, C_t \qquad 0.50 < C_t < 0.76 \qquad (10)$$

The data fitted equations (9) and (10) with a mean standard deviation of 0.19% and 0.72% respectively.

To compute the dimensionless residence time distribution function, E , for this system, the mean residence time of the jet flow had to be known. This required knowledge of the volume of the mixing chamber available to the jet flow. This volume was not the physical volume of the mixing chamber since the jet flow did not spread itself throughout the mixing chamber. Therefore, this volume was not known a priori. It was possible to estimate the maximum values of these volumes from data that was published in a paper by Barchilon and Curtet (1). In this paper, the upstream and downstream points of zero velocity for the recirculation eddy, points N and P respectively, are presented graphically on a plot of Craya-Curtet number as a function of the distance from the jet source along the mixing tube. Point P was at a fixed position for $C_t < 1$. Normalizing the distance parameter with respect to the mixing tube radius, the distance to points N and P from the jet source used in this study can then be obtained by multiplying the dimensionless distance function by the radius of the mixing tube used in the present study. The volume of the mixing chamber downstream of point N to the measuring electrodes of the conductivity probe, was considered to be available to the jet flow.

In that same paper, curves were also presented showing the jet boundary as a function of axial distance from the jet source for several valus of C_t. From these data, the radius of the jet was found at the point where the jet crossed a line drawn perpendicular to the flow through point N. To obtain these radii, it was necessary to interpolate between the given data. This was done by linear interpolation. The volume available for mixing between the jet source and point N was then calculated by assuming that this volume could be represented by the frustum of a cone. The results of these calculations are shown in Table 3. The mean residence time was then calculated by dividing the total volume available to the jet flow, V, by the total volumetric flow rate, v_t, through the system. The mean residence times thus calculated are shown as a function of C_t in Figure 16.

Mean residence times of the jet flow were also calculated using equation (4), which was dedimensionalized with the estimated mean residence time, τ. Table 4 shows a comparison between calculated dimensionless and dimensional mean residence times, $\overline{\theta}_E$ and $\overline{t}_E$ respectively, and the estimated mean residence times, τ. It must be remembered that the mean residence times that were calculated according to equation (4) include the effect of the injection time.

V_1 = Volume from the jet source to point N
V_2 = Volume from point N to point P
V_3 = Volume from point P to beginning of converging section (0.00158 cu.ft.)
V_4 = Volume within the converging section to the electrodes (0.00232 cu.ft.)
$V = V_1 + V_2 + V_3 + V_4$

C_t	Jet Radius at Point P	Distance to Point N	V_1	V_2	V	v_t	$\tau = \frac{V}{v_t}$
	in	in	$(ft)^3$	$(ft)^3$	$(ft)^3$	$(ft)^3$/sec	sec
.510	.710	3.28	.00132	.00518	.01040	.00420	2.48
.577	.756	3.71	.00166	.00440	.00996	.00472	2.11
.631	.793	4.03	.00196	.00382	.00968	.00515	1.88
.695	.837	4.40	.00235	.00315	.00940	.00563	1.67
.754	.873	4.73	.00272	.00255	.00917	.00608	1.51
.815	.908	5.09	.00314	.00189	.00893	.00654	1.37
.875	.942	5.39	.00355	.00135	.00880	.00698	1.26
.942	.980	5.79	.00409	.00062	.00861	.00748	1.15
1.009	1.000	6.13	.00449	.00000	.00839	.00796	1.05

TABLE 3 : PREDICTED MEAN RESIDENCE TIMES FOR THE CYLINDRICAL CONFINED JET ACCORDING TO DATA BY BARCHILON AND CURTET

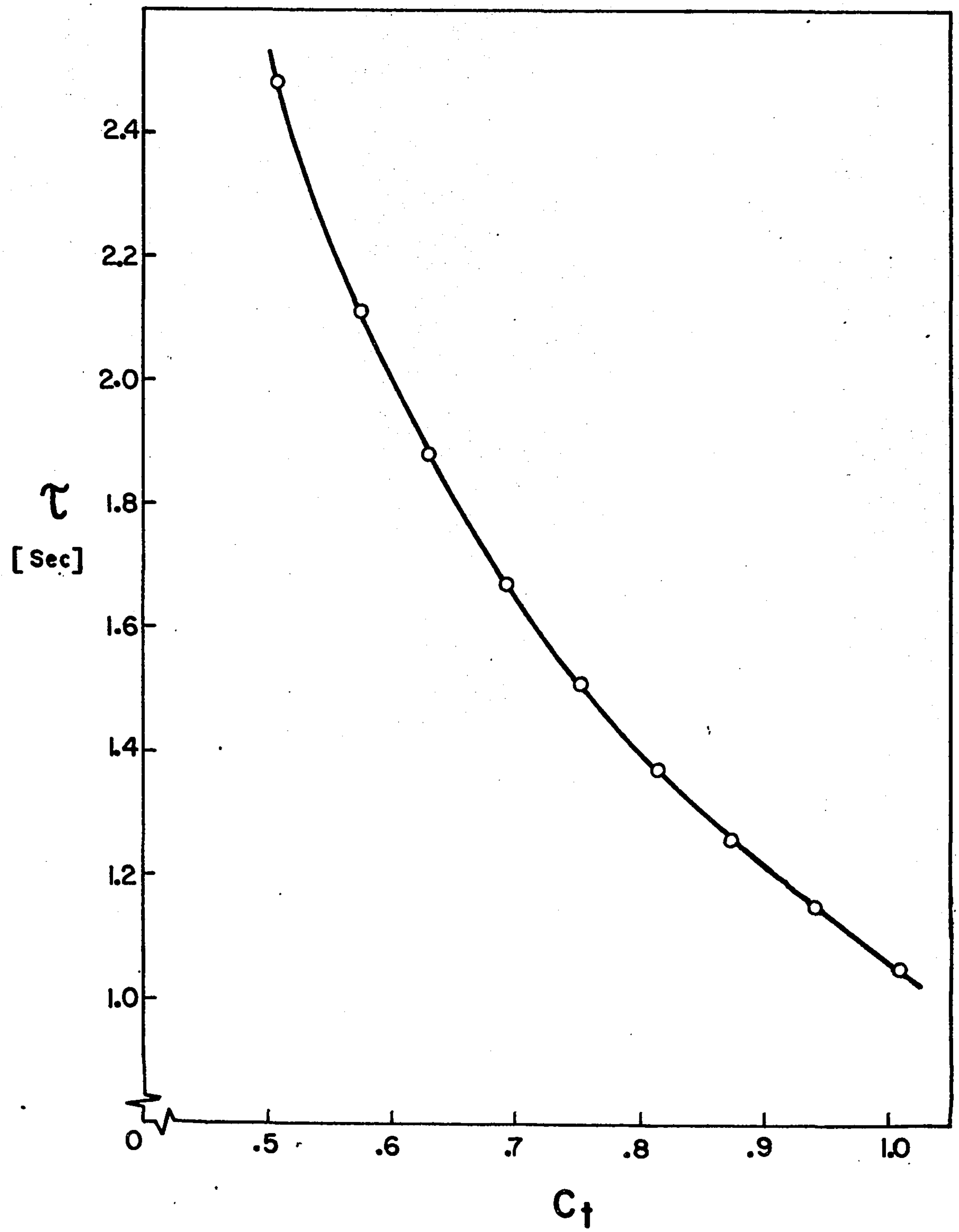

FIGURE 16 : EFFECT OF THE CRAYA - CURTET NUMBER ON THE PREDICTED MEAN RESIDENCE TIME

C_t	$\overline{\theta}_E$	$\overline{\theta}_E$	$\overline{t}_E$	τ
	$(\theta=2.5)$	$(\theta \to \infty)$	sec	sec
.510	.815	1.018	2.509	2.474
.631	.855	1.018	1.915	1.881
.815	.948	.989	1.350	1.365
1.009	1.033	1.053	1.108	1.052

TABLE 4 : COMPARISON OF ESTIMATED AND CALCULATED MEAN RESIDENCE TIMES

The dimensionless E function was calculated by use of equation (11) which is derived in Appendix 1.

$$E = \frac{C' \tau}{\int_0^\infty C' \, dt} \tag{11}$$

where C' = concentration cell monitor output as registered on the recorder

RTD curves for several values of C_t are shown in Figures 17 to 19. Figure 19 also indicates the reproducibility of the data for $C_t = 0.875$. The experimental data for these curves are shown in Appendix 11.

Some RTD curves were obtained from data taken with the mixing chamber volume decreased by 15%. This reduction in volume was achieved by sliding the converging section in the mixing chamber closer to the jet source. This was done to see what changes, if any, would occur in the RTD curves. This was also a method to see if the position of the converging section was the correct one to study only the axial mixing in the confined jet system. Figures 20 and 21 show the RTD curves for $C_t = 1.009$ and 0.695 respectively, with and without the total mixing volume decreased.

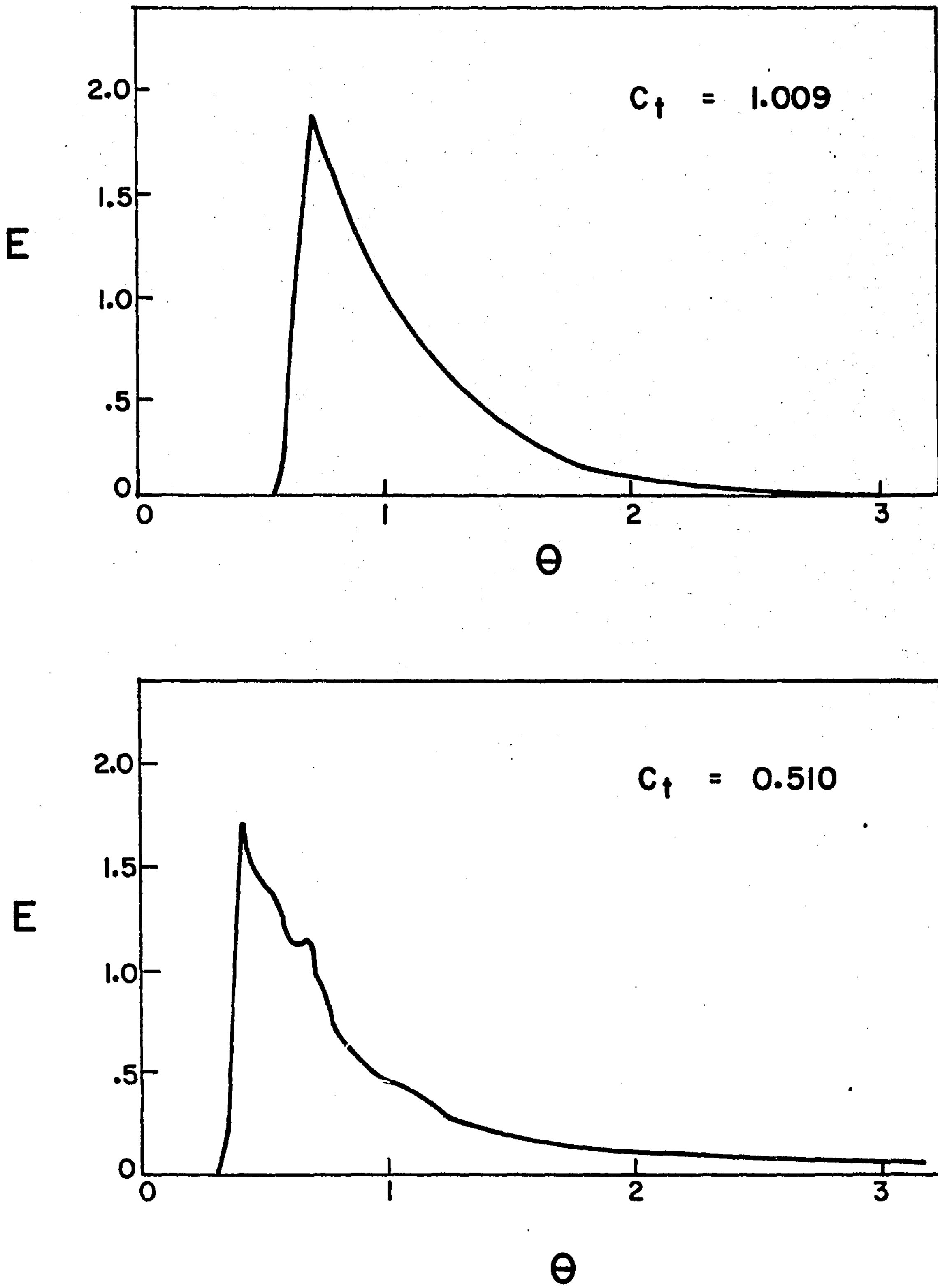

FIGURE 17 : RTD CURVES OF THE CYLINDRICAL CONFINED JET FOR C_t = 1.009 AND C_t = 0.510

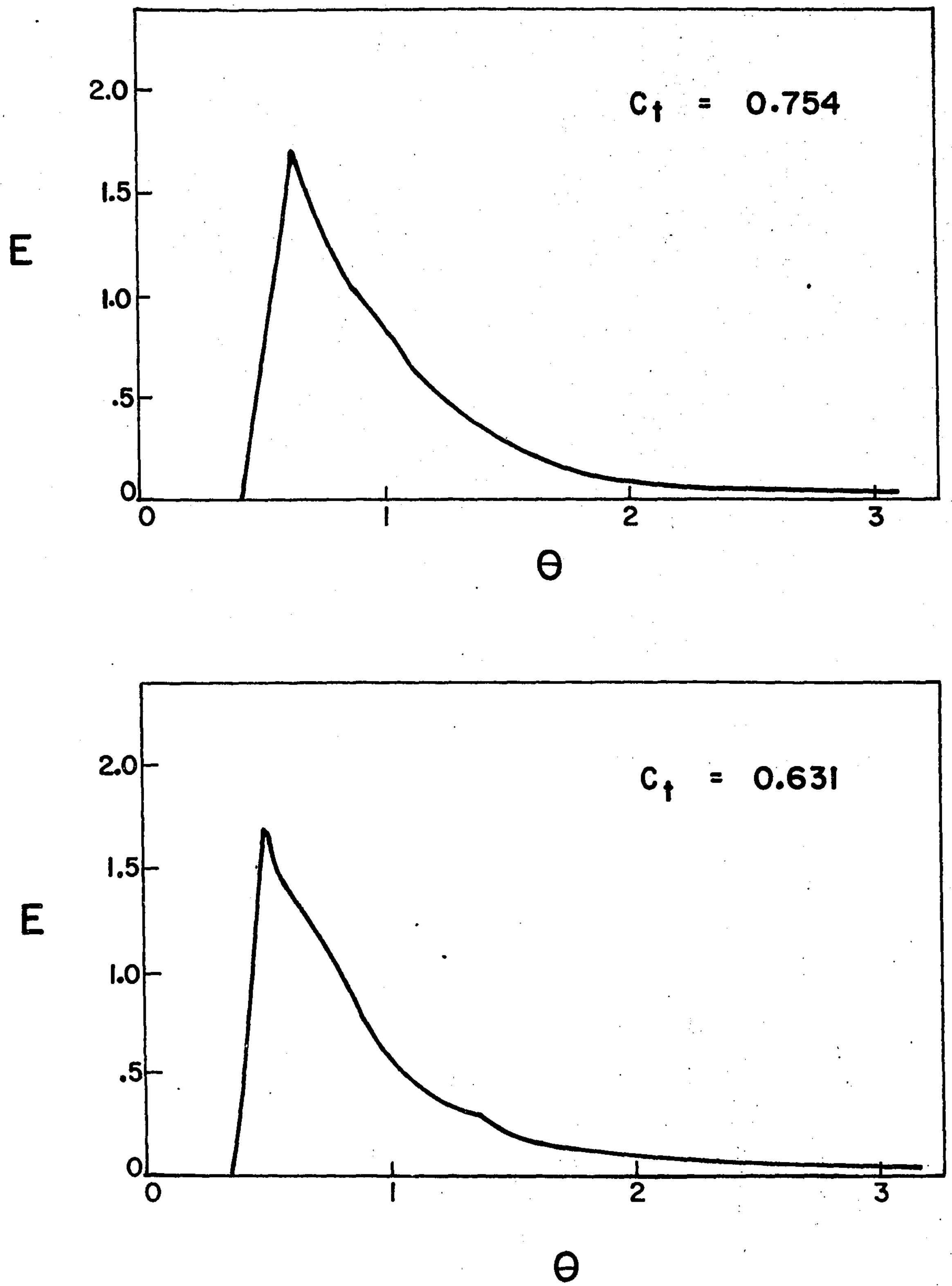

FIGURE 18 : RTD CURVES OF THE CYLINDRICAL CONFINED JET FOR C_t = 0.754 AND C_t = 0.631

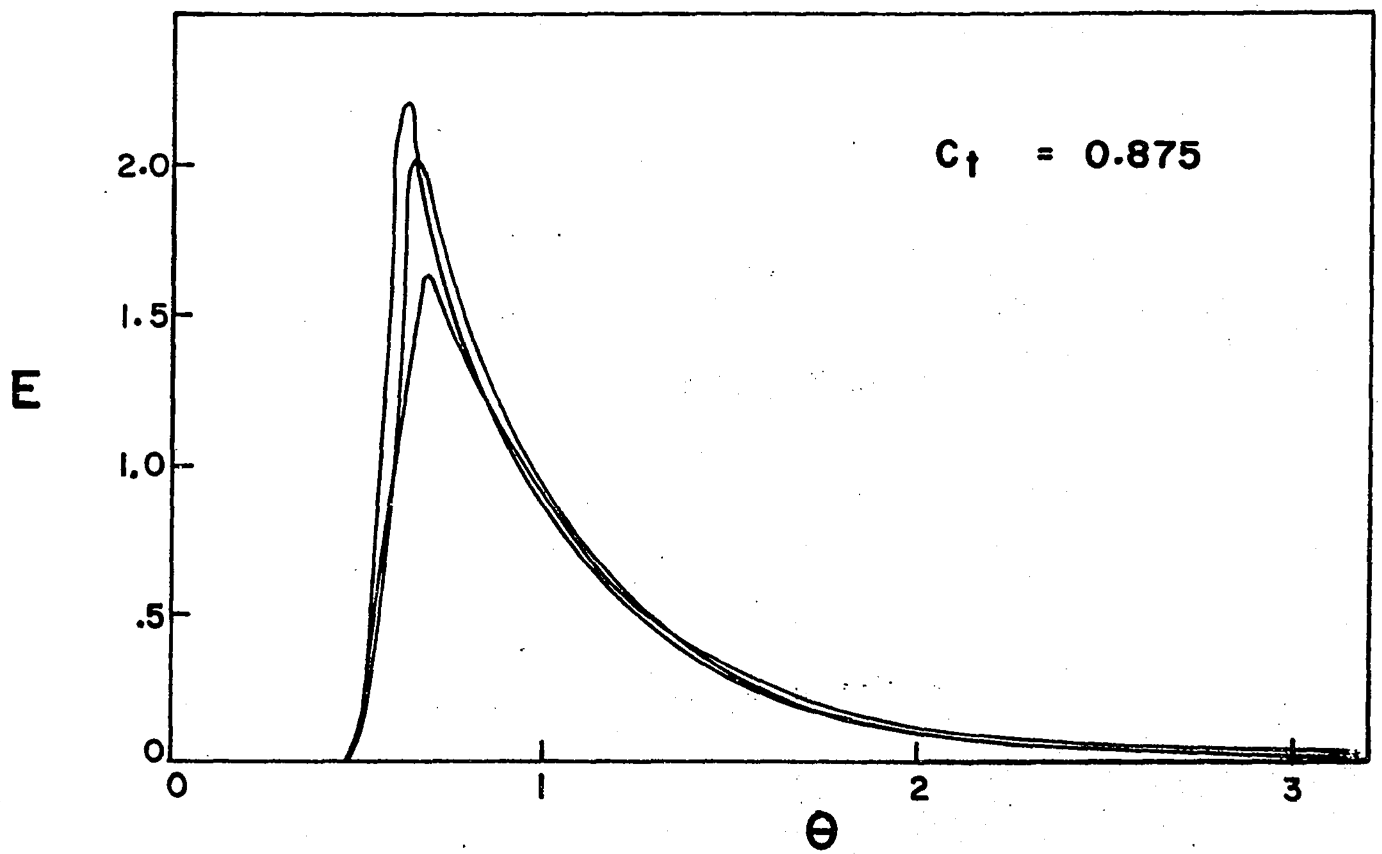

FIGURE 19 : RTD CURVES OF THE CYLINDRICAL CONFINED JET SHOWING REPRODUCIBILITY (C_t = 0.875)

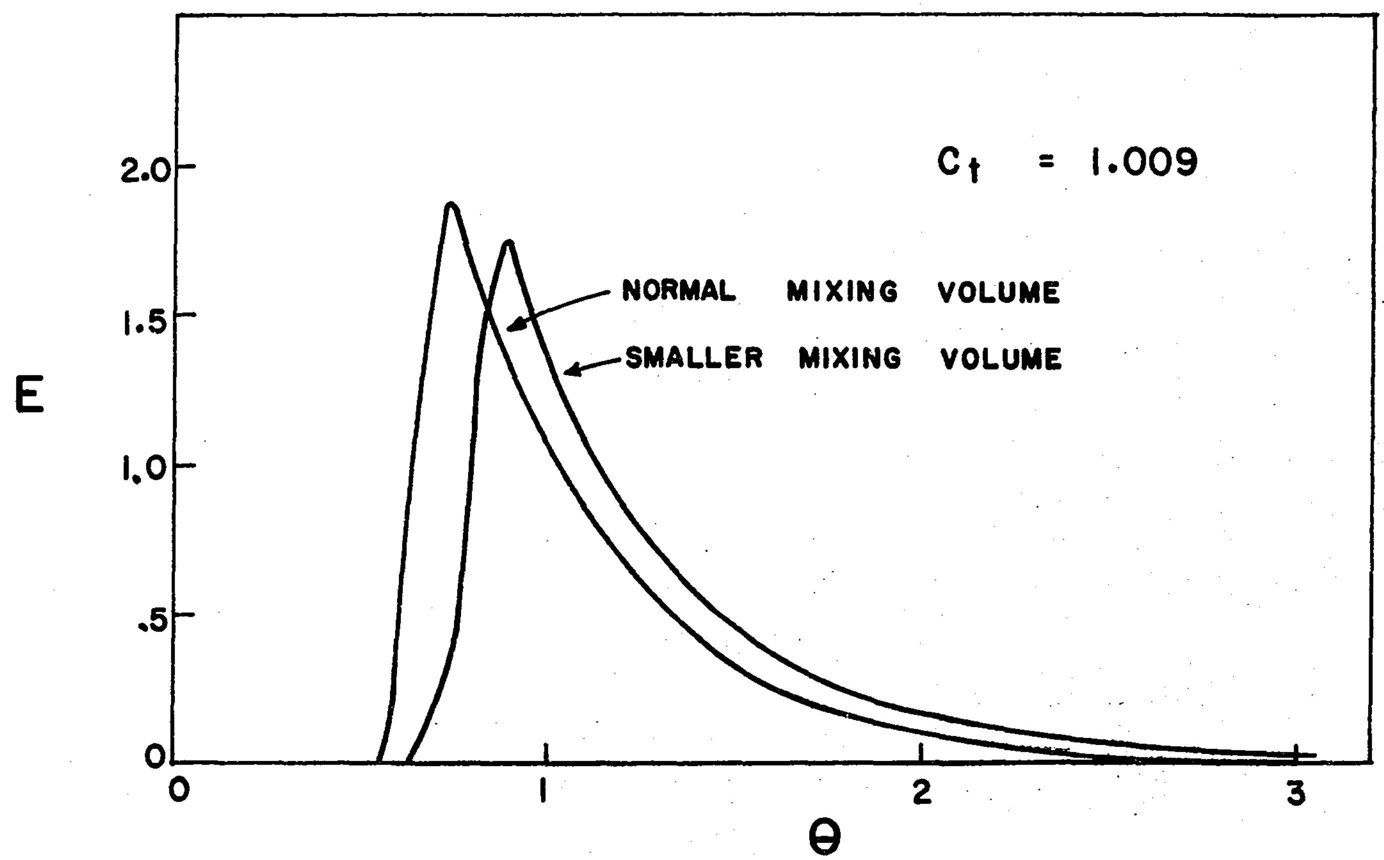

FIGURE 20: RTD CURVES OF THE CYLINDRICAL CONFINED JET WITH SMALLER MIXING VOLUME (C_t = 1.009)

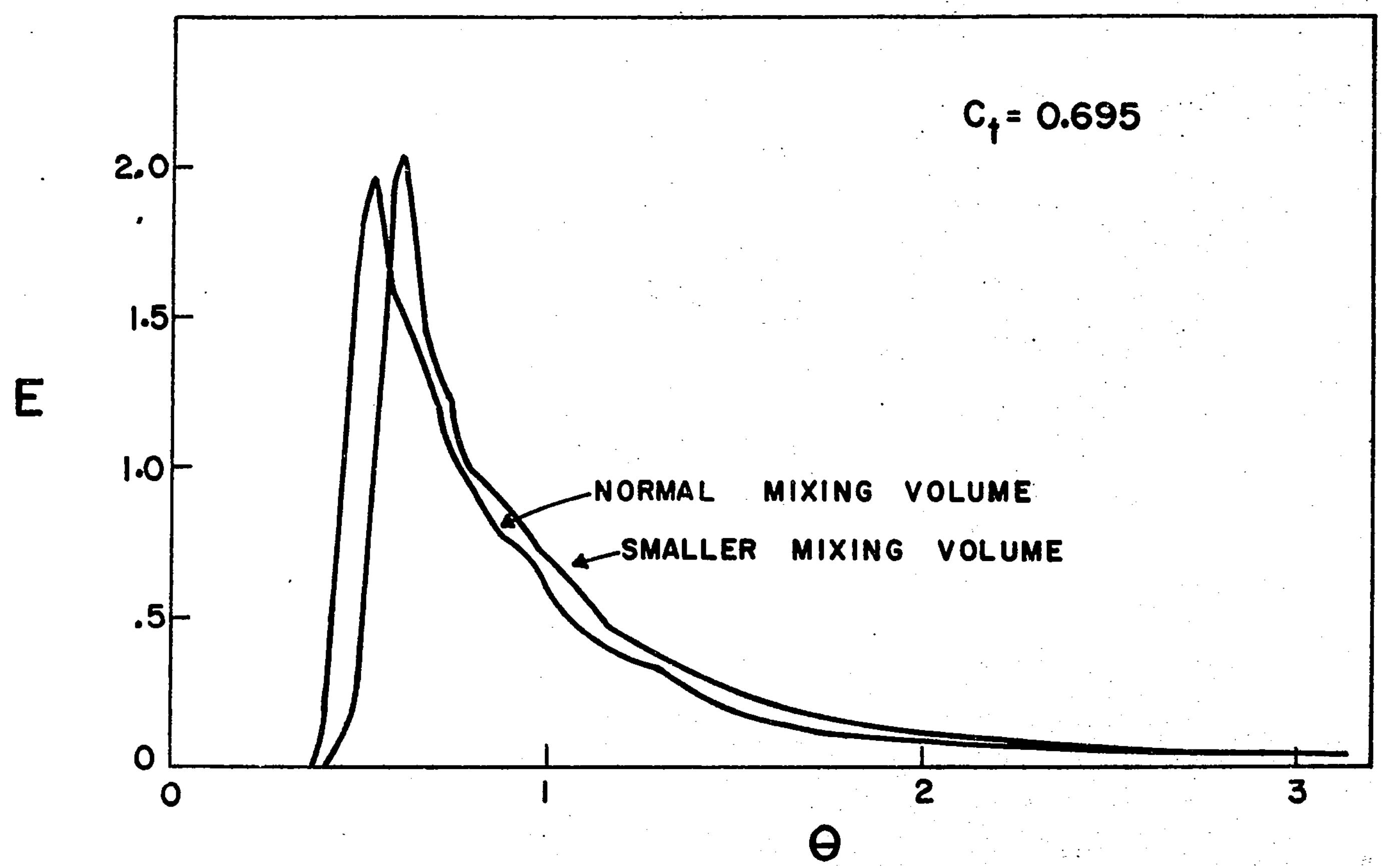

FIGURE 21 : RTD CURVES OF THE CYLINDRICAL CONFINED JET WITH SMALLER MIXING VOLUME (C_t = 0.695)

VI

DISCUSSION OF RESULTS

Typical stimulus pulses, as measured at the end of the jet tube, are shown in Figure 13. These cannot be called square pulses because of the long tails. However, these long tails cannot be attributed to the injection technique or the diffusion of the tracer solution in the jet tube. A reasonable explanation is to be found by examination of the way in which the tracer concentration in the outlet stream is measured. It was not possible to measure the tracer concentration at the end of the jet tube using available equipment. As seen in Figure 10, the fluid leaving the jet tube first entered a short divergent adapter section before flowing into the conductivity probe. Moreover, the end of the probe facing the oncoming flow provided a small mixing volume, as shown in Figure 9. Since the mean residence time of the fluid was only 0.42 seconds, any amount of tracer solution detained for even a short period of time at the mouth of the conductivity probe would cause relatively long tails on the concentration versus time curves. Thus, the pulse signals at the entrance to the mixing chamber could be assumed to be more squarish than indicated by the sample curves in Figure 13.

The effect of mixing occurring at the entrance to the conductivity probe on the output curves of the confined jet system was thought to be considerably less. Here, the mean residence time of fluid in the entrance section to the probe was very small compared with the mean residence time of the fluid in the confined jet. Also, the tracer concentrations in the outlet stream were much less since the flow rates were several times greater in this system.

The problem of estimating the mean residence time of the jet fluid without recourse to new experimental data has already been discussed in the previous chapter. Fortunately, it was possible to estimate these mean residence times from data reported in the literature (1). As shown in Table 3, the estimated mean residence times, τ, of the jet fluid in the confined jet system varied from about 1 to 2.5 seconds. The injection time was estimated to be about 0.15 ± 0.05 seconds. Thus the assumption of an ideal pulse could not be made.

If the injections could be considered to be in the form of square pulses, then the effect of the non-ideal pulse injections would be to increase the mean residence time above that calculated assuming an ideal pulse by half the time of the duration of the square pulse (12). Thus, the mean residence times, $\bar{t}_E$, that were calculated from the tracer output curves according to equation (4), would all be a little too high, since these would include the effect of the injection time.

It should be noted again that the estimated mean residence times of the jet flow, as shown in Table 3, represent the maximum mean residence times. This is true because the available mixing volume was calculated assuming that the tracer solution would spread to the extremities of the jet and recirculation eddy. However, this is not necessarily so. It is therefore not surprising that mean residence times, $\bar{t}_E$, calculated by equation (4), are less than those predicted in Table 3, taking into account the effect of the injection time, estimated to be about 0.1 seconds. A comparison between predicted and calculated mean residence times is given in Table 4. Thus it appears that it was not completely valid to dedimensionalize the experimental data with the predicted mean residence times since these are probably a little too high. However, the experimentally determined values of $\bar{t}_E$ had an error of up to $\pm 4\%$ associated with them because of inaccuracies in determining concentrations at the tail end of the output curves. Furthermore, values of $\bar{t}_E$ for the same flow condition would vary because of differences in the injection time. Therefore the estimated mean residence times were used to dedimensionalize the experimental data.

Residence time distribution curves for various values of C_t are shown in Figures 17 to 19. For convenient comparison, Figure 17 shows the RTD curves for the highest and lowest values of C_t for which data were taken. Some important conclusions may be drawn from these curves by visual inspection.

Clearly, the confined jet system becomes more "mixed" with decreasing values of C_t. This is indicated by the shift of the RTD curve to the left. This shift implies, by comparison with Figure 2, that the flow is becoming less plug-like and more like a perfectly mixed flow. Also, the increase in the length of the tail of the curve for the low value of C_t suggests greater mixing activity. Neither of the curves seem to indicate that there is any by-passing of jet fluid. However, the existence of dead space is suggested in the RTD curve for $C_t = .510$ by the long tail that persists up to $\theta = 5$. For $C_t = 1.009$, the E function becomes 0 at $\theta = 3$. Thus, although the mixedness of the system increases with decreasing values of C_t, so also does the amount of dead space in the system, which is usually undesireable. Table 4 indicates that there is dead space in the system for $C_t = .510$, amounting to about 20 % of the available mixing volume.

Another interesting aspect of the RTD curves is in the fluctuations that appear in the curves for values of C_t less than about 0.70. These fluctuations increase with decreasing values of C_t. Barchilon and Curtet (1) have observed a back and forth motion of the recirculatory eddy in this flow system. This would explain the observed phenomenon. It should be mentioned that these fluctuations are more clearly indicated when concentration is plotted as a function of actual time, in units of seconds. By dedimensionalizing the time coordinate, the fluctuations take on a very distorted appearance.

The reproducibility of the RTD curves is indicated in Figure 19 for $C_t = 0.875$. The greatest difference between these curves is in their maxima. The most representative curve for this flow condition is assumed to be the one with the highest peak for reasons discussed in Chapter V. In addition to having the highest peak, this curve also has the fastest rate of rise of the E function. Finally, the amount of tracer injected in this run was less than in the other two runs. These facts would seem to indicate that this run had the shortest injection time. The time at which the dimensionless E function first rises from zero, θ^*, and the exponential slopes of the curves are nearly the same for all of the runs.

Figure 14 shows the effect of C_t on the time delay, t^*. The relationship between these functions is linear for $C_t > 0.80$ and exponential for $C_t < 0.76$ in the range of C_t values in which data were taken. This is shown in equations (7) and (8). Figure 15 shows the effect of C_t on the exponential slope, S. The relationship between these functions is linear for all values of C_t studied, as shown in equations (9) and (10). However, a change of slope of about 10% occurs in this functional relationship in the range $0.76 < C_t < 0.80$. It is in this same range of C_t values that the relationship between t^* and C_t changes from being linear to being exponential. It is of interest to note here, that both Becker (2) and Dealy (9) have visually observed the onset of recirculation to occur for $C_t = 0.75$ and $C_t = 0.78$ respectively. Velocity profile measurements by Barchilon and Curtet (1) show that recirculation sets in for a C_t value of about 0.90. It would appear, however, according to the results of this study, that the effect of the recirculation eddy becomes significant only for values of C_t less than 0.80.

Figure 14 shows that t^* always increases with decreasing values of C_t. If θ^* (equal to t^*/τ) were plotted as a function of C_t, then θ^* would steadily decrease with decreasing values of C_t. This can be observed in Figures 17 to 19. The function, θ^*, is an indicator of the role of plug flow in this system. As θ^* approaches zero, the system approaches a state of perfect mixing. As θ^* approaches one, the system approaches a state of simple plug flow.

Figure 15 shows that S always decreases as C_t decreases. The inverse of the slope S gives the mean residence time of an equivalent "perfectly mixed region".

Thus, the smaller the value of C_t, the greater the mixedness of the fluid in this system. The increase in the mixedness of the system corresponds to the decrease in the plug flow state of the system.

A study of RTD curves was carried out with the mixing chamber volume decreased by 15 %. The decrease in volume was achieved by placing the converging section in the mixing chamber closer to the jet source. The estimated available mixing volume of the jet flow for the system with decreased mixing volume was calculated by subtracting that volume by which the mixing chamber was decreased from the predicted available volumes presented in Table 3, for a particular value of C_t. The RTD curves that were obtained in this study are shown in Figures 20 and 21. For easy comparison, RTD curves for the system with the normal mixing chamber volume are also presented on the same graphs. The curves in the above figures show that the system becomes less mixed when the total available mixing volume was decreased. This effect was greater for high C_t than for low C_t.

To understand the effect on the system when the available mixing volume is reduced, one must first look at how the mixing volume was chosen initially. As explained earlier, the volume of the mixing chamber was adjusted visually by dye injections so that for the highest value of C_t studied, the jet would spread to the mixing tube wall before entering the converging section leading to the conductivity probe. The reason for this was that it was only of interest to study axial mixing in the confined jet system, not downstream pipe mixing. In practice, the entrance to the converging section was placed at a distance of 3/4" downstream from the point where the dye first reached the mixing tube wall. This was to make certain that the converging section would not interfere with the jet's development to the mixing tube wall. The further downstream from the point where the jet spreads to the wall the outlet tracer concentration is measured, the more the mixing in the confined jet system will be masked by downstream pipe mixing. On the other hand, the converging section had to be far enough downstream so as not to affect the boundary conditions, as used in the theoretical analysis of the cylindrical confined jet.

When the mixing chamber volume was decreased, the position of the adjustable converging section within the mixing chamber became such that it interfered with the jet's development. It was no longer possible for the jet to spread to the mixing tube wall before entering the converging section for high C_t. For low C_t, the converging section interfered with the normal flow pattern of the recirculation eddy.

To give physical significance to the results of this investigation, it is useful to interpret the RTD curves in terms of a mixing model. For $C_t = 1.009$, the data curves can be reproduced accurately by a plug flow tank and perfect mixer in series, with a square pulse signal input. From such a model, the plug flow volume and the perfectly mixed volume can be calculated from t^* and S respectively. For the system with the normal mixing chamber volume, the total available mixing volume for the jet flow is 0.00836 cu.ft., as calculated from the experimental data in terms of the mixing model. The estimated volume is 0.00837 cu.ft. for this case. With the mixing chamber volume decreased by 15%, the total available mixing volume for the jet flow is 0.00697 cu.ft. as calculated from the experimental data in terms of the mixing model and the estimated mixing volume is 0.00622 cu.ft. The fact that the experimentally determined volume was considerably greater than the estimated one for the case of decreased mixing chamber volume, seems to indicate that the boundary conditions of the confined jet system have been affected by the decrease in the mixing chamber volume. This change in the boundary conditions seems to have affected the flow pattern in this system by increasing the angle of spread of the jet. This would result in a larger available mixing volume. This description is consistent with the experimental data.

For $C_t = 0.695$, the effect of decreasing the mixing volume on the RTD curve was less than for $C_t = 1.009$. This is to be expected since for the high value of C_t mixing is occurring more or less evenly throughout the system, but for the low value of C_t , a great part of the mixing is concentrated in the recirculation eddy. Thus, by decreasing the mixing volume at low C_t , the state of mixing in the system is not as much affected. The simple mixing model of a plug flow tank and perfect mixer in series does not apply for low values of C_t so that a simple quantitative interpretation cannot be made.

This investigation clearly shows that the mixing chamber volume used in this study was the correct one for investigating axial mixing in a cylindrical confined jet. By decreasing this volume, the boundary conditions are affected so that it is no longer known what system one is studying. By increasing this volume, one no longer studies only the mixing in a confined jet, but also pipe mixing, which was not of interest.

A schematic diagram of the hypothesized mixing process in the cylindrical confined jet system is given in Figure 22 . The mixing process is suggested by the experimental data and from the known fluid dynamics of cylindrical confined jets. The mixing regions, as shown, are not necessarily in the physical order that the fluid encounters them in the flow through the system because the mixing regions all overlap. For example, the jet flow does

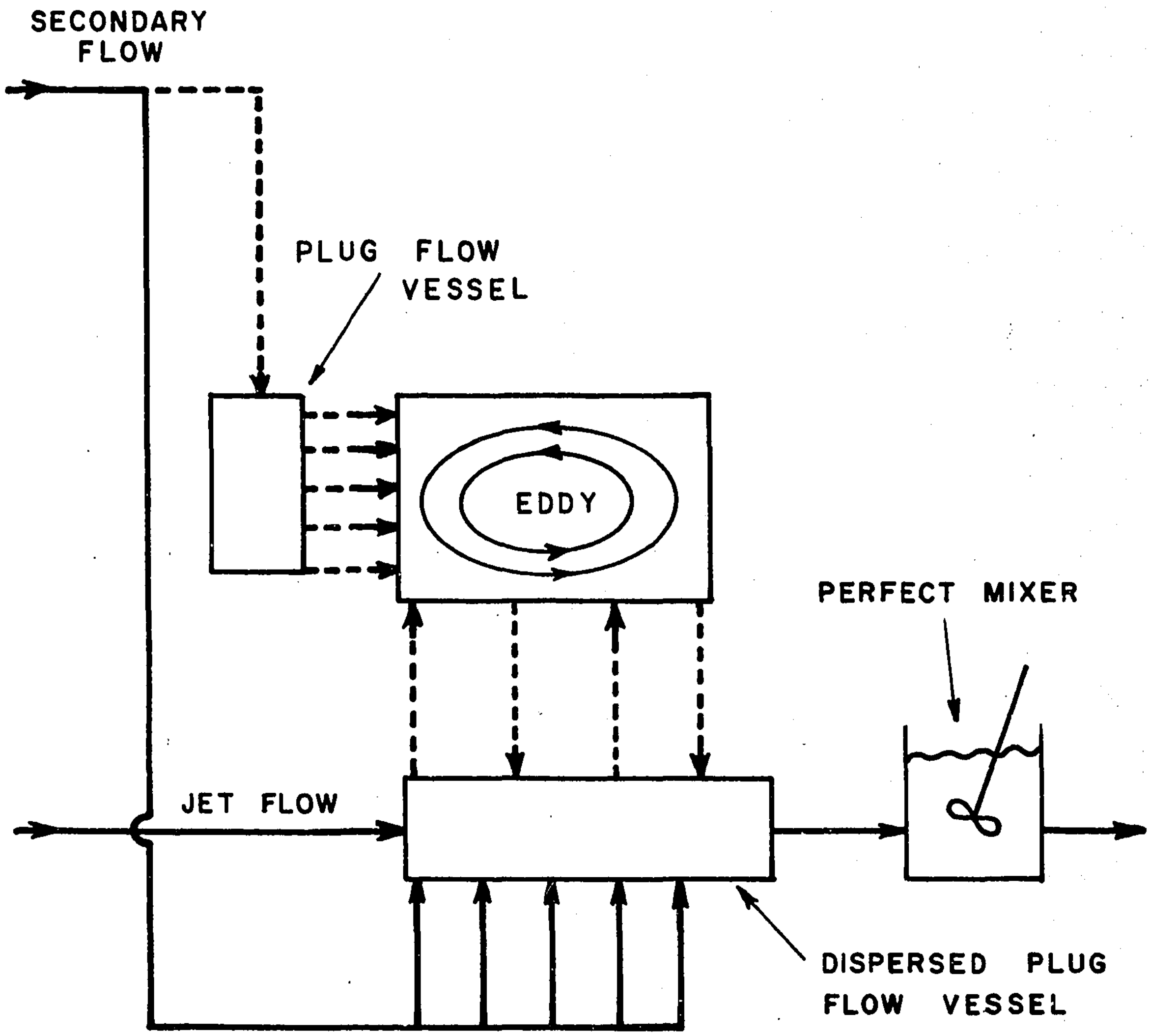

FIGURE 22 : SCHEMATIC DIAGRAM OF THE HYPOTHESIZED MIXING PROCESS IN A CYLINDRICAL CONFINED JET

not actually enter a dispersed plug flow region followed by a perfectly mixed region, but both regions exist simultaneously. The mixing processes occur in parallel and not in series. There are really two mixing patterns involved depending on whether there is recirculation or not.

For flows without recirculation, the flow is along the solid lines only. Since the recirculation eddy does not exist, the model is greatly simplified. The secondary flow combines with the jet flow in a continuous manner, but at different times and positions along the developing jet. Thus, part of the total available mixing volume is in dispersed plug flow and the other part is perfectly mixed as indicated by the perfectly mixed tank.

With the onset of recirculation, the flow complexity is greatly increased. The secondary flow is divided, with some of the fluid mixing directly with the fluid in the recirculation eddy, at different times, and the rest of the fluid mixing with the jet flow as before. Some of the fluid mixture of jet and secondary flow is drawn continuously into the recirculation eddy, to be returned to the main flow after a certain time delay. This is indicated in the RTD curves. For low values of C_t, these curves are exponential in character having a constant slope for times up to about 4 seconds. For times greater than this, the slope of the exponential suddenly decreases to a considerably lower constant value. Such a change in slope indicates an increase in the mixedness of the system which is the expected effect of the recirculation eddy.

Representation of this picture of the flow in the form of a mathematical model would be extremely difficult. Figure 23 shows a simplified mixing model of the cylindrical confined jet, suitable for the establishment of a mathematical model that might be adequate for predicting, for example, the performance of this system as a chemical reactor. This model varies in complexity depending on whether recirculation exists or not. Solid lines show the model for flow without recirculation. Dotted lines become actual flow lines when recirculation occurs.

For non-recirculatory flows, the model simply consists of a plug flow region and a perfectly mixed region in series. Both mixing region volumes can be calculated from the experimental data, and the two flow rates are known. This model is consistent with the RTD curves obtained experimentally.

For recirculatory flows, two unknown flow rates and three more mixing regions are introduced. As a first approximation, all mixing region volumes can be estimated making use of the experimental data, the physical boundaries of the system, and the data published by Barchilon and Curtet (1). This leaves two unknown flow rates for the system, both of which are functions of C_t. This model could be tested on a hybrid computer using square pulse inputs.

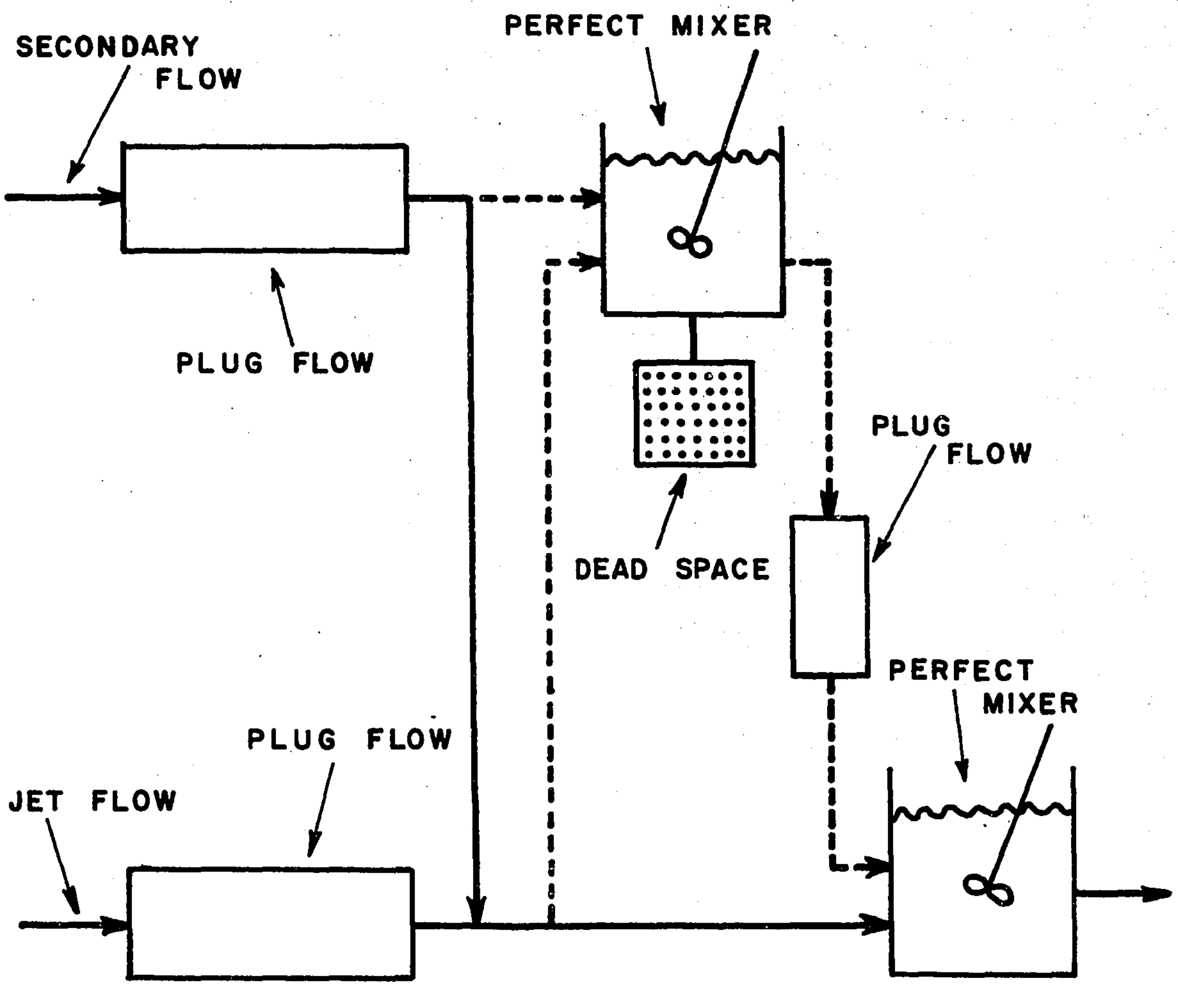

FIGURE 23 : SIMPLIFIED MIXING MODEL OF THE CYLINDRICAL CONFINED JET

VII

CONCLUSIONS AND RECOMMENDATIONS

In this investigation, the mixing of fluid in a cylindrical confined jet was studied for flows with and without recirculation. In particular, the residence time distributions were obtained by a tracer study in the range of C_t values from about 0.50 to 1.10. Several parameters of the RTD curves were correlated with C_t. The simplicity of these relationships points out the fundamental significance of the similarity parameter, C_t.

The results of this investigation show that the recirculation eddy becomes effective in the mixing process only for values of C_t less than 0.80. Also, with an increase in the recirculation rate in the eddy, the amount of dead space in the confined jet system increases considerably. Nearly 20% of the mixing volume available to the jet flow can be considered to be dead space for $C_t = 0.510$. Thus, when the mixedness of the fluid in the system is increasing because of the increase in the recirculation rate in the eddy, the amount of dead space also increases. Hence, the cylindrical confined jet, by itself, does not seem very effective as a mixer of different fluids for industrial purposes. However, this type of flow system may be useful as a chemical reactor for autocatalytic and autothermal reactions because in these reactions recycle flow is often desirable (13).

To obtain a more accurate picture of the mixing process occurring in this system, reproducible RTD data should be obtained. This might be done by automating the injection technique using a quick-acting solenoid valve controlled by a timer that is accurate in the range of 100 milli-seconds. This would eliminate the human factor from the experimental technique so that the data would lend themselves to a statistical analysis. Such data could be used to test the mixing model that has been proposed for this system.

If the stimulus pulses are such that these are not easily reproduced on a computer, it might be possible to measure the RTD of the jet flow directly at the jet source. This would make it possible to account for the shape of the stimulus pulse using the convolution integral. This method has been described by Moser and Cupit (16) using a hybrid computer and by Gwyn (11) using a digital computer.

Studies to date have dealt with a single fluid, usually water or air, in both jet and secondary flows. It would be of interest, both theoretical and experimental, to study the mixing process in a confined jet using a different fluid in the jet than in the secondary. This would be of practical importance in jet flame furnaces and other reacting systems.

NOMENCLATURE

Symbol	Meaning
C	tracer concentration in the outlet stream
C'	concentration cell monitor output as registered on the recorder
C_o	initial concentration of a pulse injection if all the tracer material was evenly distributed throughout the available mixing volume
C_t	Craya-Curtet number (defined in equation (2))
D_1	jet source diameter
D_2	mixing tube diameter
E	exit age distribution function of fluid leaving a vessel, or the residence time distribution of a fluid in a vessel
I	internal age distribution function of a fluid in a vessel
L	specific conductance
m	Curtet's similarity parameter
m_o	initial value of m (defined in equation (1))
N	upstream point of zero velocity at the boundary of the recirculation eddy
P	downstream point of zero velocity at the boundary of the recirculation eddy

Symbol	Meaning
Q	total mass of tracer injected
R_1	jet source radius
R_2	mixing tube radius
S	initial slope of the tracer output curves when plotted on semi-logarithmic paper
t	time
t^*	time interval from when the tracer first enters the mixing chamber to when it first leaves it
$\bar{t}_E$	mean residence time (defined in equation (4))
t_o	time when the tracer first enters the mixing chamber
t'	point of the recorder curve indicating the completion of a pulse injection
U_1	jet source velocity
U_2	secondary flow velocity at jet source
V	total volume available to the jet flow
V_t	total volumetric flow rate in the mixing tube
θ	reduced time (defined by equation (5))
θ^*	dimensionless time delay
τ	mean residence time
Λ_o	equivalent conductance at infinite dilution

REFERENCES

1. Barchilon, M., and Curtet, R., "Some Details of the Structure of an Axisymmetric Confined Jet with Back-Flow", ASME Publ., No. 64-FE-23, (1964)

2. Becker, H.A., Hottel, H.C., and Williams, G.C., "Mixing and Flow in Ducted Turbulent Jets", Ninth Symposium on Combustion - 1962, 7, Academic Press, (1963).

3. Bischoff, K.B., "Mixing and Contacting in Chemical Reactors", Industrial and Engineering Chemistry, 58, 11, (1966).

4. Bischoff, K.B., and McCracken, E.A., "Tracer Tests in Flow Systems", Industrial and Engineering Chemistry, 58, 7, (1966).

5. Cholette, A., and Cloutier, L., "Mixing Efficiency Determinations for Continuous Flow Systems", Canadian Journal of Chemical Engineering, 37, 3, (1959).

6. Curtet, R., "Sur l'Ecoulement d'un Jet Entre Parois", Publ. Scientifiques et Techniques du Ministere de l'Air, No. 359, (1960).

7. Curtet, R., "Confined Jets and Recirculation Phenomena in Cold Air", Combustion and Flame, 2, 4, (1958).

8. Danckwerts, P.V., "Continuous Flow Systems-Distribution of Residence Times", Chemical Engineering Science, 2, 1, (1953).

9. Dealy, J. M., Momentum Exchange in a Confined Circular Jet with Turbulent Source, Ph.D. Thesis, University of Michigan, (1963).

10. Dixon, D.C., and Roper, G. H., "Residence-time Distributions in Cylindrical Tanks with Axial Inlet and Outlet", Institution of Engineers, Australia, Mechanical and Chemical Engineering Transactions MC 2, 2, (Nov. 1966).

11. Gwyn, J. E., "Digital Resolution of Residence Time Distributions from Pulse Response Data", Preprint 23 B, Sixty-Third National Meeting, A.I.Ch.E., (Feb. 1968).

12. Hill, P. M., M.Eng. Thesis, McMaster University, Canada, (1964).

13. Levenspiel, O., Chemical Reaction Engineering, John Wiley and Sons, Inc., New York, (1962).

14. Levenspiel, O., and Bischoff, K. B., "Patterns of Flow in Chemical Process Vessels", Advances in Chemical Engineering, 4, (1963).

15. Mayer, E. A., "Confined Jet Amplifier", ASME Publ., No. 67-WA/FE-14, (1967).

16. Moser, J. H., and Cupit, C. R., "Resolving RTD's with Hybrid Computers", Chemical Engineering Progress, 62, 6, (1966).

17. Spalding, D. B., "A Note on Mean Residence Times in Steady Flows of Arbritary Complexity", Chemical Engineering Science, 9, 1, (1958).

APPENDIX I

Determination of the Tracer Recovery in the Efflux

The material balance on the tracer material is given by the equation :

$$Q = \int_0^\infty C \, v_t \, dt \tag{12}$$

where Q is the total mass of tracer material injected, C is the concentration of the tracer material in the outlet stream defined by equation (6) and v_t is the total volumetric flow rate in $(ft)^3$/sec. Changing the concentration units to gm/$(ft)^3$, removing the constant terms out from under the integral sign and substituting equation (6), equation (12) becomes :

$$Q = \frac{16.65 \times 10^5 \, v_t}{\Lambda_o} \int_0^\infty L \, dt \tag{13}$$

The output from the recorder is in terms of voltage as a function of time. The relationship between the voltage and the conductivity is given by the expression :

$$1 \text{ mv} = 10^{-4} \text{ mhos/cm} \tag{14}$$

and therefore

$$\int_0^{\infty} L \; dt = 10^{-4} \int_0^{\infty} C' \; dt \tag{15}$$

where C' is the concentration cell monitor output as registered on the recorder, in units of mv. On substituting equation (15) into equation (13), the material balance becomes :

$$Q = \frac{165.5 \; v_t}{\Lambda_o} \int_0^{\infty} C' \; dt \tag{16}$$

Λ_o is evaluated under the operating temperature by a method described in the International Critical Tables, Volume 6 . The area under a recorder curve, $\int_0^{\infty} C' \; dt$, is measured with a planimeter, and v_t is experimentally known from the rotameters. The material recovered, Q , is given in units of grams.

Derivation of the E Function

The dimensionless E function for a pulse injection can be shown to be given by the relation :

$$E = \frac{C}{C_o} \tag{17}$$

where C_o is the initial concentration of the injected tracer material, if evenly distributed throughout the available mixing volume. Values of C are related to

C by the equation :

$$C = \frac{0.1\ C'}{\Lambda_o} \tag{18}$$

Recalling equation (12) and substituting equation (18), we have :

$$C_o = \frac{Q}{V} = \frac{1}{V} \int_0^\infty \frac{v_t\ 0.1\ C'\ dt}{\Lambda_o} \tag{19}$$

Substituting equations (18) and (19) into equation (17), we obtain, after cancelling like terms, the equation :

$$E = \frac{C'}{\int_0^\infty C'\ dt} \times \frac{V}{v_t} \tag{20}$$

or, recalling the definition of the mean residence time, τ , we have the equation :

$$E = \frac{C'\ \tau}{\int_0^\infty C'\ dt} \tag{11}$$

APPENDIX II

RTD Data for the Cylindrical Confined Jet

$C_t = 1.009$	$\int_0^\infty C'dt = .724$ mv-sec		$\tau = 1.052$ sec
t	C'	E	θ
sec	mv		
.58	0.00	0.000	.546
.61	.09	.130	.580
.65	.44	.640	.618
.70	.90	1.308	.665
.75	1.185	1.722	.713
.78	1.285	1.867	.737
.80	1.23	1.787	.760
.85	1.10	1.598	.808
.90	1.00	1.453	.856
.95	.87	1.265	.903
1.00	.81	1.177	.951
1.05	.725	1.053	.998
1.10	.645	.937	1.046
1.15	.58	.843	1.093
1.20	.55	.800	1.141
1.30	.44	.654	1.236
1.40	.34	.494	1.331
1.50	.255	.370	1.426
1.60	.215	.312	1.521
1.70	.17	.247	1.616
1.80	.14	.203	1.711
2.00	.085	.123	1.901
2.25	.05	.073	2.139
2.50	.03	.044	2.376
2.75	.02	.029	2.614

Data with Normal Mixing Volume ($C_t = 1.009$)

C_t = .875 $\int_0^\infty C'dt$ = 1.330 mv-sec τ = 1.259 sec

t	C'	E	θ
sec	mv		
.59	0.00	0.000	.469
.65	.11	.104	.516
.70	.35	.331	.556
.75	.98	.928	.596
.80	2.035	1.926	.635
.82	2.125	2.014	.651
.85	2.050	1.940	.675
.90	1.76	1.666	.715
.95	1.69	1.600	.755
1.00	1.55	1.467	.794
1.05	1.36	1.288	.834
1.10	1.34	1.269	.874
1.15	1.185	1.122	.913
1.20	1.05	.993	.953
1.25	.90	.852	.993
1.30	.89	.842	1.033
1.35	.82	.777	1.072
1.40	.725	.686	1.112
1.45	.675	.640	1.152
1.50	.60	.568	1.191
1.60	.505	.478	1.271
1.70	.39	.369	1.350
1.80	.345	.326	1.430
1.90	.29	.274	1.509
2.00	.245	.232	1.589
2.25	.145	.137	1.787
2.50	.09	.085	1.986
2.75	.06	.057	2.184
3.00	.045	.040	2.383
3.50	.02	.019	2.780
4.00	.01	.009	3.177

Data with Normal Mixing Volume (C_t = .875)

C_t = .875	$\int_0^\infty C'dt$ = 1.198 mv-sec		τ = 1.259
t	C'	E	θ
sec	mv		
.60	0.00	0.000	.477
.65	.115	.121	.516
.70	.715	.752	.556
.75	1.96	2.060	.596
.80	2.10	2.207	.631
.85	1.69	1.776	.675
.90	1.55	1.629	.715
.95	1.39	1.460	.755
1.00	1.325	1.392	.794
1.05	1.215	1.277	.834
1.10	1.13	1.187	.874
1.15	1.015	1.066	.913
1.20	.935	.982	.953
1.25	.845	.888	.993
1.30	.795	.836	1.033
1.35	.75	.788	1.072
1.40	.675	.709	1.112
1.45	.605	.636	1.152
1.50	.57	.599	1.191
1.60	.47	.494	1.271
1.70	.35	.368	1.350
1.80	.305	.321	1.430
1.90	.25	.263	1.509
2.00	.235	.247	1.589
2.10	.185	.194	1.668
2.20	.15	.157	1.747
2.50	.09	.094	1.986
2.75	.05	.053	2.184
3.00	.04	.042	2.383
3.50	.02	.021	2.780
4.00	.015	.016	3.177

Data with Normal Mixing Volume (C_t = .875)

$C_t = .875$	$\int_0^\infty C'dt = 1.412$ mv-sec	$\tau = 1.259$ sec	
t	C'	E	θ
sec	mv		
.61	0.00	0.000	.488
.65	.15	.134	.516
.70	.65	.580	.556
.75	.96	.856	.596
.80	1.30	1.159	.635
.85	1.81	1.614	.675
.90	1.76	1.569	.715
.95	1.60	1.427	.755
1.00	1.465	1.306	.794
1.10	1.34	1.195	.874
1.20	1.15	1.025	.953
1.30	.86	.767	1.033
1.40	.80	.713	1.172
1.50	.65	.580	1.191
1.60	.54	.481	1.271
1.70	.45	.401	1.350
1.80	.39	.348	1.430
2.00	.28	.250	1.589
2.25	.19	.169	1.787
2.50	.14	.125	1.986
2.75	.09	.080	2.184
3.00	.07	.062	2.383
3.50	.04	.036	2.780
4.00	.03	.031	3.177
4.50	.02	.018	3.574

Data with Normal Mixing Volume ($C_t = .875$)

C_t = .754	$\int_0^\infty C' dt$ = 1.250 mv-sec		τ = 1.507 sec
t	C'	E	θ
sec	mv		
.63	0.00	0.000	.419
.70	.25	.301	.464
.75	.525	.633	.498
.80	.785	.946	.531
.85	.97	1.169	.564
.90	1.20	1.447	.597
.95	1.40	1.688	.630
1.00	1.34	1.616	.664
1.05	1.24	1.495	.697
1.10	1.135	1.368	.730
1.15	1.08	1.302	.763
1.20	1.01	1.218	.796
1.25	.94	1.133	.829
1.30	.875	1.055	.863
1.40	.81	.977	.929
1.50	.715	.862	.995
1.60	.60	.723	1.062
1.70	.515	.621	1.128
1.80	.45	.543	1.194
2.00	.35	.422	1.327
2.20	.25	.301	1.460
2.40	.19	.229	1.593
2.60	.14	.169	1.725
2.80	.10	.121	1.858
3.00	.075	.090	1.991
3.25	.06	.072	2.157
3.50	.05	.060	2.322
4.00	.025	.030	2.654
4.25	.018	.021	2.820

Data with Normal Mixing Volume (C_t = .754)

$C_t = .695$	$\int_0^\infty C'dt = 2.103$ mv-sec		$\tau = 1.670$ sec
t	C'	E	θ
sec	mv		
.63	0.00	0.000	.377
.65	.12	.095	.389
.70	.68	.540	.419
.75	1.395	1.108	.449
.80	1.835	1.457	.479
.85	2.255	1.791	.509
.88	2.455	1.950	.530
.90	2.435	1.934	.539
.95	2.095	1.664	.569
1.00	1.895	1.505	.599
1.05	1.855	1.473	.629
1.10	1.715	1.362	.659
1.15	1.555	1.235	.689
1.20	1.355	1.076	.719
1.25	1.250	.993	.749
1.30	1.220	.969	.778
1.35	1.105	.877	.808
1.40	1.020	.810	.838
1.45	.97	.770	.868
1.50	.955	.758	.898
1.55	.94	.746	.928
1.60	.855	.679	.958
1.65	.715	.568	.988
1.70	.69	.548	1.018
1.75	.665	.528	1.048
1.80	.585	.465	1.078
1.90	.515	.409	1.138
2.00	.490	.389	1.198
2.10	.455	.361	1.257
2.20	.395	.314	1.317
2.30	.34	.270	1.377
2.40	.29	.230	1.437
2.50	.25	.199	1.497
2.60	.20	.159	1.557
2.80	.15	.119	1.677
3.00	.135	.107	1.796
3.20	.105	.083	1.916
3.50	.085	.066	2.096
3.75	.075	.060	2.246
4.00	.068	.054	2.395
4.50	.055	.044	2.695
5.00	.050	.040	2.994

Data with Normal Mixing Volume ($C_t = .695$)

C_t = .631	$\int_0^\infty C'dt$ = 2.449 mv-sec		τ = 1.881 sec
t	C'	E	θ
sec	mv		
.66	0.000	0.000	.351
.70	.065	.050	.372
.75	.325	.250	.399
.80	.86	.660	.425
.85	1.45	1.114	.452
.90	1.82	1.398	.478
.95	2.135	1.640	.505
.96	2.14	1.644	.510
1.00	2.05	1.574	.532
1.05	1.915	1.471	.558
1.10	1.85	1.420	.585
1.15	1.80	1.383	.611
1.20	1.75	1.345	.638
1.25	1.675	1.287	.665
1.30	1.59	1.221	.691
1.35	1.575	1.209	.718
1.40	1.52	1.168	.744
1.45	1.40	1.076	.771
1.50	1.35	1.036	.797
1.55	1.34	1.029	.824
1.60	1.185	.910	.851
1.65	1.04	.799	.877
1.70	1.00	.767	.904
1.75	1.00	.767	.930
1.80	.875	.672	.957
1.85	.80	.615	.984
1.90	.74	.568	1.010
2.00	.64	.491	1.063
2.10	.55	.423	1.116
2.20	.52	.399	1.170
2.30	.445	.342	1.223
2.40	.42	.322	1.276
2.50	.40	.307	1.329
2.60	.375	.288	1.382
2.80	.275	.211	1.489
3.00	.225	.173	1.595
3.50	.14	.108	1.861
4.00	.105	.081	2.127
4.50	.073	.056	2.392
5.00	.055	.042	2.658
5.50	.05	.038	2.924

Data with Normal Mixing Volume (C_t = .631)

C_t = .510	$\int_0^\infty C'dt$ = 1.805 mv-sec		τ = 2.474 sec
t	C'	E	θ
sec	mv		
.72	0.000	0.000	.291
.75	.013	.017	.303
.80	.10	.137	.323
.85	.335	.460	.344
.90	.64	.878	.364
.95	.915	1.254	.384
1.00	1.14	1.564	.404
1.03	1.24	1.700	.418
1.05	1.21	1.658	.424
1.10	1.105	1.514	.445
1.15	1.07	1.467	.465
1.20	1.02	1.398	.485
1.25	1.00	1.371	.505
1.30	.99	1.356	.525
1.35	.98	1.343	.546
1.40	.92	1.262	.566
1.45	.855	1.173	.586
1.50	.83	1.138	.606
1.55	.825	1.131	.626
1.60	.84	1.150	.647
1.65	.825	1.131	.667
1.70	.755	1.034	.687
1.75	.70	.960	.707
1.80	.675	.925	.728
1.85	.62	.849	.748
1.90	.55	.755	.768
2.00	.505	.693	.808
2.10	.455	.623	.849
2.20	.405	.554	.889
2.40	.34	.465	.970
2.80	.275	.376	1.132
3.00	.22	.302	1.213
3.50	.16	.219	1.415
4.00	.13	.178	1.617
4.50	.09	.123	1.819
5.50	.083	.113	2.021
6.00	.063	.086	2.425
7.00	.043	.058	2.829
8.00	.035	.048	3.234

Data with Normal Mixing Volume (C_t = .510)

$C_t = 1.009$	$\int_0^\infty C'dt = .784$ mv-sec		$\tau = .782$ sec
t	C'	E	θ
sec	mv		
.49	0.000	0.000	.627
.55	.175	.175	.703
.60	.57	.569	.767
.65	1.51	1.506	.831
.69	1.75	1.746	.882
.75	1.45	1.446	.959
.80	1.27	1.267	1.023
.85	1.125	1.122	1.087
.90	.95	.948	1.151
.95	.84	.838	1.215
1.00	.75	.748	1.279
1.05	.64	.638	1.343
1.10	.55	.549	1.407
1.15	.485	.484	1.471
1.20	.435	.434	1.535
1.30	.325	.324	1.662
1.40	.26	.259	1.790
1.50	.20	.199	1.918
1.60	.165	.165	2.046
1.80	.105	.105	2.302
2.00	.065	.065	2.558
2.25	.038	.038	2.877
2.50	.015	.015	3.197

Data with Smaller Mixing Volume ($C_t = 1.009$)

C_t = .695	$\int_0^\infty C' dt$ = 1.367 mv-sec		τ = 1.287 sec
t	C'	E	θ
sec	mv		
.53	0.00	0.000	.412
.60	.09	.085	.466
.65	.48	.452	.505
.70	1.28	1.205	.544
.75	2.015	1.897	.583
.78	2.16	2.034	.602
.80	2.06	1.939	.622
.85	1.65	1.553	.660
.90	1.42	1.337	.699
.95	1.315	1.238	.738
1.00	1.065	1.003	.777
1.10	.97	.913	.856
1.20	.87	.819	.932
1.30	.71	.668	1.010
1.40	.61	.574	1.088
1.50	.49	.461	1.166
1.60	.44	.414	1.243
1.80	.335	.315	1.399
2.00	.25	.235	1.554
2.25	.165	.155	1.748
2.50	.13	.122	1.943
3.00	.08	.075	2.331
3.50	.05	.047	2.720
4.00	.035	.033	3.108

Data with Smaller Mixing Volume (C_t = .695)